Fast and Continual Learning for Hybrid Control Policies using Generalized Benders Decomposition

Xuan Lin†

***Abstract*— Hybrid model predictive control with both continuous and discrete variables is widely applicable to robotic control tasks, especially those involving contact with the environment. Due to the combinatorial complexity, the solving speed of hybrid MPC can be insufficient for real-time applications. In this paper, we proposed a hybrid MPC solver based on Generalized Benders Decomposition (GBD). The algorithm enumerates and stores cutting planes online inside a finite buffer. After a short cold-start phase, the stored cuts provide warm-starts for the new problem instances to enhance the solving speed. Despite the disturbance and randomly changing environment, the solving speed maintains. Leveraging on the sparsity of feasibility cuts, we also propose a fast algorithm for Benders master problems. Our solver is validated through controlling a cart-pole system with randomly moving soft contact walls, and a free-flying robot navigating around obstacles. The results show that with significantly less data than previous works, the solver reaches competitive speeds to the off-the-shelf solver Gurobi despite the Python overhead.**

I. Introduction

Hybrid model predictive control (Hybrid MPC) with both continuous and discrete variables is widely applicable to robotic control tasks, especially those involving contact with the environment. However, discontinuous variables are oftentimes computed offline for Hybrid MPC [1]–[4] due to their combinatorial complexities. These include gaits for legged robots and contact sequences for manipulation tasks. Several models with mixed discrete-continuous variables were proposed including mixed-logic dynamic systems (MLDs) [5], linear complementary models (LCs) [6], and piecewise affine systems (PWAs) [7]. Their conditional equivalences were established in [8] (for example, LCs are equivalent to MLDs provided that the complementary variables are bounded). Several recent works focus on solving Hybrid MPC on these systems [9]–[11] including contact sequences. Despite their works showing potential, it is always beneficial to further increase the solving speed such that the controller can react promptly under noise and model errors.

In this paper, we propose a novel hybrid MPC solver based on Generalized Benders decomposition (GBD) [12] to solve problems including MLD constraints under changing environments. Benders decomposition separates the problem into a master problem which solves part of the variables named complicating variables, and a subproblem which solves the rest of the variables. It uses a delayed constraint generation technique that builds up representations of the feasible region and optimal cost function for complicating variables inside the master problem. These representations are constructed as cutting planes based on the dual solutions of the subproblem. The key idea we propose is to store the cuts inside a finite buffer as more problem instances are solved, since the dual feasible set is invariant under the changing environments. The stored cuts then provide warm-starts for new problem instances, significantly increasing the solving speeds. In the best scenario, GBD only needs to solve one master problem and one subproblem to get a globally optimal solution. In addition, we show the data efficacy of our algorithm. At the scale of the problems we studied, GBD needs much less data coming from solved problems to find good warm-starts than previous works [13]. Therefore, GBD has potential to quickly learn warm-starts online to deal with out-of-distribution cases, or when the system dynamics are undetermined before the solver begins (for example, the robot may have an unknown payload until it is handed over). The proposed solver is compared against the recent works on warm-started Branch-Bound solvers and the commercialized solver Gurobi.

We list the contributions below:

1) We propose a novel algorithm based on GBD for Hybrid MPCs, where the cuts are stored online which provide warm-starts for the new problem instances to increase solving speeds, and
2) We propose a novel algorithm utilizing the sparsity of feasibility cuts to solve the Benders master problem, and
3) We propose a technique to accelerate the cold-start process by shifting feasibility cuts in time, and
4) We tested our solver on controlling a free-flying robot navigating around obstacles, and a cart-pole system with randomly moving soft contact walls. The latter problem is more challenging than cart-pole with static walls prevail in previous literature [9], [11], [14], [15]. We show that our GBD solver runs at competitive speeds to off-the-shelf solver Gurobi despite the Python overhead. For the cart-pole experiment, GBD often exceeds Gurobi.

Compared to the previous version [16], we improved the scaling up performance of contribution 1, added contribution 2, and supplied more experiments in contribution 4. While contribution 2, 3 rely on problems having dynamic constraints, contribution 1 does not and can be applied to general parametric optimization problems.

The rest of this paper is organized as follows. Section III presents the Hybrid MPC problem with MLD models. Section IV applies GBD to solve MLD models and describe

†Xuan Lin is with Department of Mechanical and Aerospace En- gineering, University of California, Los Angeles, CA 90095 USA {xuanlin1991}@gmail.com

the basic GBD algorithm including shifted cuts. Section V describes how warm-starts are generated and stored with some theoretical analysis. Section VI describes an algorithm for Benders master problem utilizing sparse feasibility cuts. Section VII conducts experiments on an inverted pendulum with moving soft-contact walls and a free-flying robot navigating around obstacles. Section VIII concludes the paper and discusses the results and future directions.

Notations Vectors are bold lowercase; matrices are bold uppercase; sets are script or italicized uppercase. The real number set is $\mathbb{R}$. For $\boldsymbol{x}, \boldsymbol{y} \in \mathbb{R}^n$, $\boldsymbol{x} \leq \boldsymbol{y}$ indicates element-wise inequality. For $\boldsymbol{A} \in \mathbb{R}^{n\times n}$ and $\boldsymbol{B} \in \mathbb{R}^{m\times m}$, $\text{diag}(\boldsymbol{A}, \boldsymbol{B}) \in \mathbb{R}^{(n+m)\times(n+m)}$ denotes the block diagonal matrix with diagonal blocks $\boldsymbol{A}$ and $\boldsymbol{B}$, and zeros otherwise. $\boldsymbol{I}_n$ denotes an identity matrix of dimension n. $\boldsymbol{1}_n$ denotes a vector of all ones of dimension n. The open ball $B_\epsilon(\boldsymbol{p})$ denotes $\{\boldsymbol{q} : ||\boldsymbol{p} - \boldsymbol{q}|| < \epsilon\}$. The cone $A_\alpha(\boldsymbol{p})$ denotes $\{\boldsymbol{q} : \text{angle}(\boldsymbol{p}, \boldsymbol{q}) < \alpha\}$. Throughout the paper, we use square brackets to denote the time step for variables such as [k].

II. Related Works

A. Mixed-Logic Dynamic Models (MLDs)

In [5], the authors proposed mixed-logic dynamics systems as a general modeling tool for control systems incorporating physical laws, logic rules and operating constraints. MLD is rich enough to incorporate dynamic systems such as finite state machines, nonlinear systems that can be written as piece-wise linear form. MLDs have been widely used to model energy storage systems [17], transportation systems [18], temperature management systems [19], to name a few. Recently, MLDs and its equivalent models such as linear complementary models are introduced into the robotics locomotion and manipulation community to model real-time control involving contacts [9]–[11], [13].

MLDs incorporate states and inputs that can be a mixture of continuous and discrete variables, and quadratic objective functions. Since MLDs incorporate a mixture of discrete and continuous variables, solving it online for fast motion planning and model-predictive control demands an efficient MIQP solver. Several methods have been proposed including explicit MPC [20], Branch-and-Bound [11], ADMM [9], Lagrange relaxation [21], elastic modes [22], and generalized Benders decomposition [23]. We briefly go over them below.

Explicit MPC solves the problem completely or partially offline, such that the solver only picks out solutions online. [24] building polyhedron regions of invariant optimal control function for LQR problems. Explicitly building polytope regions is computationally expensive hence limited to simple problems. [25] stored all solutions and used a K-nearest-neighbor approach to pick out binary solutions. [20] explored a partial explicit approach that combines offline solved binary solutions with online convex computation. Related to this work is the library building approach where the problem is solved offline and recorded into a dataset. The solver then picks out data points and uses them as warm-starts. The online data selection approach can be a K-nearest neighbor classifier [26], [27], or a learned neural-network [13]. However, this approach generally has difficulty facing out-of-distribution scenarios from the dataset. Except for [11], the works mentioned above only use offline optimal solutions. The infeasible or suboptimal solutions are not used.

Branch and bound is a common approach to solve mixed-integer programs used by off-the-shelf solvers such as Gurobi. This approach first relaxes the integer programming problem into a convex programming on the root node where all binaries are extended to continuous variables between zero and one. It then fixes the binary variables one-by-one, and generate branches from the root to a solution on the leaf node where all binary variables are fixed. Previous studies tried to use information from previous solve to warm-start the new solve online. [28] studied propagating the path from root to leaf from the previous iteration to the next one for warm-start, such that a number of parent nodes do not need to be resolved. [11] further explored propagating complete B&B tree to warm-start the next problem. Even with the proposed techniques, B&B can still be slow as it has too many subproblems to keep track of, particularly under noise and model inaccuracies.

Another approach to solve mixed-integer programs is through the alternating direction method of multipliers (ADMM). ADMM solves two or multiple problems iteratively until they reach a consensus through a penalty in the objective function. It is applicable to many kinds of problems: QPs[29], MIPs[9], or even MINLPs[30], [31]. Computer vision and operation research community has used ADMM to solve large scale MIP problems [32]. In the robotics community, ADMM has been implemented for solving complementary control problems [9] at a fast speed. Despite [9] does not discuss it, ADMM allows for easy warm-start [29], using the previous solution to accelerate the solving of the next solution. On the other hand, ADMM does not have convergence guarantees for MIP problems unless special assumptions are made such as [32].

B. Benders Decomposition

Benders decomposition [33] can be regarded as Danzig-Wolfe decomposition [34] applied to the dual. Both of them use delayed column or constraint generation techniques. Benders decomposition identifies the complicating variables and defines a subproblem such that those variables are fixed. For this technique to work well, the subproblem should be much easier to solve than the complete problem. For mixed-integer programming, the subproblem is the convex part with complicating variables being the discrete variables [23]. As subproblems are solved, cutting planes are added to the master problem to build the feasible set and optimal cost function for the subproblem.

Benders decomposition was originally proposed to solve linear duals e.g. MILPs. In [12], the author proposed Generalized Benders decomposition (GBD) that extends the theory to nonlinear duals. Several authors have investigated solving MIQPs using GBD [23], [35]–[37]. In [38], [39], the authors propose logic-based Benders decomposition which further

generalized the theory to so-called inference dual, which is a logic combination of propositions. This method extends the application of BD to planning and scheduling problems such as satisfiability of 0-1 programming problems whose dual is not a traditional linear or nonlinear programming problem. Using this idea, [40] proposed a formulation of combinatorial Benders feasibility cut for MILPs that does not depend on the big-M constant.

As Benders decomposition involves master-subproblem structure, it suits the large-scale distributed problems, or problems with a large number of possible scenarios like stochastic programs [41]. For applications such as distributed control [42], the subproblems can be decoupled into multiple smaller-scale problems and solved in parallel to reduce the computation demand. As pointed out by the review paper [43], many authors report over 90% solving time spent on the master problem. Therefore, a number of previous work investigated on how to speed up the master problem, or use its results more efficiently. Examples include local branching heuristics [44], heuristic master problem solutions [45], generating pareto-optimal cuts [46], cut initialization [47], valid inequalities [48], etc. See [43] for a comprehensive review of these methods. [49] points out that classic Benders feasibility cuts do not carry objective function value leading to convergence issues. They proposed additional feasibility cuts to resolve this issue.

Benders cuts can also be used to learn objective functions. This has been applied to dual dynamic programming for MPC over long-term problems [50], [51]. Previous work [52], [53] uses Benders cuts to construct lower bounds for infinitely long objective functions using Bellman operators for both nonlinear and mixed-integer linear systems. Through learning Benders cuts from offline dataset, one avoids hand-tuning terminal cost of objective function. Despite a more optimal objective being learned, the online solving speed of MIP is invariant of objective functions.

III. Problem Model

We develop MPC control laws for Mixed Logic Dynamic (MLD) systems as proposed by [5]:

$$\boldsymbol{x}[k+1] = \boldsymbol{E}\boldsymbol{x}[k] + \boldsymbol{F}\boldsymbol{u}[k] + \boldsymbol{G}\boldsymbol{\delta}[k] + \boldsymbol{n}[k] \tag{1a}$$
$$\boldsymbol{H}_1\boldsymbol{x}[k] + \boldsymbol{H}_2\boldsymbol{u}[k] + \boldsymbol{H}_3\boldsymbol{\delta}[k] \leq \boldsymbol{\theta} \tag{1b}$$

At time k, $\boldsymbol{x}[k] \in \mathbb{R}^{n_x}$ is the continuous state. $\boldsymbol{u}[k] \in \mathbb{R}^{n_u}$ denotes the continuous input. $\boldsymbol{\delta}[k] \in \{0,1\}^{n_\delta}$ is the binary input. $\boldsymbol{n}[k] \in \mathbb{R}^{n_x}$ is the disturbance input. Matrices representing system dynamics are $\boldsymbol{E} \in \mathbb{R}^{n_x \times n_x}$, $\boldsymbol{F} \in \mathbb{R}^{n_x \times n_u}$, $\boldsymbol{G} \in \mathbb{R}^{n_x \times n_\delta}$. $\boldsymbol{H}_1 \in \mathbb{R}^{n_c \times n_x}$. $\boldsymbol{H}_2 \in \mathbb{R}^{n_c \times n_u}$. $\boldsymbol{H}_3 \in \mathbb{R}^{n_c \times n_\delta}$. The submatrices are of appropriate dimensions. The right-hand side of the constraint (1b) is $\boldsymbol{\theta} \in \mathbb{R}^{n_c}$ to represent the changing environments, where n_c is the number of inequality constraints. We assume that matrices $\boldsymbol{E}$, $\boldsymbol{F}$, $\boldsymbol{G}$, $\boldsymbol{H}_1$, $\boldsymbol{H}_2$, $\boldsymbol{H}_3$ are independent of $\boldsymbol{\delta}[k]$ and $\boldsymbol{\theta}$. This makes $\boldsymbol{\delta}[k]$ and $\boldsymbol{\theta}$ as inputs to the system while the inherent physics of the system is invariant.

Remark 1. *The goal of parameter $\boldsymbol{\theta}$ can represent a sudden change in the environment that the controller is uninformed of and cannot prepare for it down the MPC horizon. Note this is different from the time-varying system investigated by [11] where the controller is well-informed of the change in advance ($\boldsymbol{\theta}_t, t = 0, ..., T$ is known).*

We formulate a hybrid MPC for this system. The MPC formulation solves an optimization problem to get a sequence of control inputs. However, only the first one is used. It then takes the sensor feedback and resolves the problem. If this could be done fast enough on the hardware, the control can reject disturbances. The MPC formulation is:

$$\begin{aligned}
\underset{\boldsymbol{x}[k]\in X_k,\ \boldsymbol{u}[k],\ \boldsymbol{\delta}[k]}{\text{minimize}} \quad & \sum_{k=0}^{N-1} (||\boldsymbol{x}[k] - \boldsymbol{x}_g[k]||^2_{\boldsymbol{Q}_k} + ||\boldsymbol{u}[k]||^2_{\boldsymbol{R}_k}) + \\
& ||\boldsymbol{x}[N] - \boldsymbol{x}_g[N]||^2_{\boldsymbol{Q}_N} \\
\text{s.t.} \quad & \boldsymbol{x}[0] = \boldsymbol{x}_{in} \\
& \boldsymbol{x}[k+1] = \boldsymbol{E}\boldsymbol{x}[k] + \boldsymbol{F}\boldsymbol{u}[k] + \boldsymbol{G}\boldsymbol{\delta}[k] \\
& \boldsymbol{H}_1\boldsymbol{x}[k] + \boldsymbol{H}_2\boldsymbol{u}[k] + \boldsymbol{H}_3\boldsymbol{\delta}[k] \leq \boldsymbol{\theta} \\
& \boldsymbol{\delta}[k] \in \{0,1\}^{n_\delta},\ k = 0, ..., N-1
\end{aligned}$$

Where $\boldsymbol{x}_g[k]$ represents the control target for $\boldsymbol{x}[k]$. The matrices $\boldsymbol{Q}_k$ and $\boldsymbol{Q}_N$ are positive definite matrices. X_k is the domain of $\boldsymbol{x}[k]$. The system is written into a more compact form:

$$\begin{aligned}
\underset{\boldsymbol{x}\in X,\ \boldsymbol{\delta}}{\text{minimize}} \quad & ||\boldsymbol{x} - \boldsymbol{x}_g||^2_{\boldsymbol{Q}} \\
\text{s.t.} \quad & \boldsymbol{A}\boldsymbol{x} = \boldsymbol{b}(\boldsymbol{x}_{in}, \boldsymbol{\delta}) \\
& \boldsymbol{C}\boldsymbol{x} \leq \boldsymbol{d}(\boldsymbol{\theta}, \boldsymbol{\delta}) \\
& \boldsymbol{\delta}_k \in \{0,1\}^{n_\delta}
\end{aligned} \tag{2}$$

Let $n_{xu} = n_x + n_u$. With a slight abuse of notation, we use $\boldsymbol{x}$ without time index $[k]$ to denote a concatenation of $\boldsymbol{x}[k]$ and $\boldsymbol{u}[k]$, and $\boldsymbol{\delta}$ denoting a concatenation of $\boldsymbol{\delta}[k]$. They have structures:

$$\begin{aligned}
&\boldsymbol{x} \in \mathbb{R}^{Nn_{xu}+n_x} \\
&= \begin{bmatrix} \boldsymbol{x}[0]^T & \boldsymbol{u}[0]^T & \cdots & \boldsymbol{x}[N-1]^T & \boldsymbol{u}[N-1]^T & \boldsymbol{x}[N]^T \end{bmatrix}^T \\
&\boldsymbol{\delta} = \begin{bmatrix} \boldsymbol{\delta}^T[0] & \cdots & \boldsymbol{\delta}^T[N-1] \end{bmatrix}^T \in \mathbb{R}^{Nn_\delta}
\end{aligned} \tag{3}$$

$$\boldsymbol{A} = \begin{bmatrix}
\boldsymbol{I}_{n_x} & \boldsymbol{0} & & & & \\
-\boldsymbol{E} & -\boldsymbol{F} & \boldsymbol{I}_{n_x} & \boldsymbol{0} & & \\
& & -\boldsymbol{E} & -\boldsymbol{F} & \ddots & \\
& & & & \ddots & \boldsymbol{I}_{n_x} \quad \boldsymbol{0} \\
& & & & & -\boldsymbol{E} \quad -\boldsymbol{F} \quad \boldsymbol{I}_{n_x}
\end{bmatrix} \tag{4}$$
$$\in \mathbb{R}^{(N+1)n_x \times (Nn_{xu}+n_x)}$$

$$\begin{aligned}
&\boldsymbol{b}(\boldsymbol{x}_{in}, \boldsymbol{\delta}) \in \mathbb{R}^{(N+1)n_x} \\
&= \begin{bmatrix} \boldsymbol{x}_{in}^T & (\boldsymbol{G}\boldsymbol{\delta}[0])^T & \cdots & (\boldsymbol{G}\boldsymbol{\delta}[N-1])^T \end{bmatrix}^T
\end{aligned} \tag{5}$$

$$\boldsymbol{C} = \begin{bmatrix} \boldsymbol{H}_1 & \boldsymbol{H}_2 & & & \\ & \boldsymbol{H}_1 & \boldsymbol{H}_2 & & \\ & & \ddots & & \\ & & & \boldsymbol{H}_1 & \boldsymbol{H}_2 & \boldsymbol{0} \end{bmatrix} \in \mathbb{R}^{Nn_c \times (Nn_{xu}+n_x)} \tag{6}$$

$$\begin{aligned} &\boldsymbol{d}(\boldsymbol{\theta}, \boldsymbol{\delta}) \in \mathbb{R}^{Nn_c} \\ &= \begin{bmatrix} (\boldsymbol{\theta} - \boldsymbol{H}_3\boldsymbol{\delta}[0])^T & \cdots & (\boldsymbol{\theta} - \boldsymbol{H}_3\boldsymbol{\delta}[N-1])^T \end{bmatrix}^T \end{aligned} \tag{7}$$

$$\boldsymbol{Q} = \text{diag}(\boldsymbol{Q}_k, \boldsymbol{R}_k) \in \mathbb{R}^{(Nn_{xu}+n_x)\times(Nn_{xu}+n_x)} \tag{8}$$

The domain of $\boldsymbol{x}$ is $X = X_k \times \mathbb{R}^{n_u} \times \cdots \times \mathbb{R}^{n_u} \times X_k$. $\boldsymbol{x}_g$ has the same structure to $\boldsymbol{x}$. We also define a concatenation of parameters as $\boldsymbol{\Theta}$:

$$\boldsymbol{\Theta} = \begin{bmatrix} \boldsymbol{x}_{in}^T & \boldsymbol{\theta} & \cdots & \boldsymbol{\theta} \end{bmatrix}^T \in \mathbb{R}^{n_x + Nn_c} \tag{9}$$

Problem (2) is an MIQP and can be solved through an off-the-shelf mixed-integer convex programming solver based on Branch and Bound, such as Gurobi. However, Branch and Bound algorithms keep track of a large number of subproblems that relax the binary constraints in different ways. Despite the MPC warm-start scheme such as shifting contact sequence can be used [11], many subproblems still need to be solved for a new problem instance. For applications that require extremely fast solving speed, this can be insufficient. In this paper, we propose to use GBD to solve (2), such that the number of solved subproblems is reduced.

IV. Benders decomposition formulation

In this section, we apply Benders decomposition to our hybrid MPC problem (2). Benders decomposition deals with the problem of the following form:

$$\begin{aligned} \underset{\boldsymbol{x},\boldsymbol{y}}{\text{minimize}} \quad & f(\boldsymbol{x}, \boldsymbol{y}) \\ \text{s.t.} \quad & \boldsymbol{G}(\boldsymbol{x}, \boldsymbol{y}) \leq 0 \\ & \boldsymbol{x} \in X, \boldsymbol{y} \in Y \end{aligned} \tag{10}$$

where $\boldsymbol{y}$ is a vector of complicating variables. If $\boldsymbol{y}$ is fixed, the optimization problem is much easier to solve. Benders decomposition partitions the problem into a master problem by projecting onto the $\boldsymbol{y}$ space:

$$\begin{aligned} \underset{\boldsymbol{y}}{\text{minimize}} \quad & v(\boldsymbol{y}) \\ \text{s.t.} \quad & \boldsymbol{y} \in Y \cap V \end{aligned} \tag{11}$$

The function $v(\boldsymbol{y})$ is defined to provide the best objective function with fixed complicating variable $\boldsymbol{y}$:

$$\begin{aligned} v(\boldsymbol{y}) = \underset{\boldsymbol{x}}{\text{infimum}} \quad & f(\boldsymbol{x}, \boldsymbol{y}) \\ \text{s.t.} \quad & \boldsymbol{G}(\boldsymbol{x}, \boldsymbol{y}) \leq 0 \\ & \boldsymbol{x} \in X \end{aligned} \tag{12}$$

where V contains all $\boldsymbol{y}$'s such that problem (12) is feasible:

$$V = \{\boldsymbol{y} : \boldsymbol{G}(\boldsymbol{x}, \boldsymbol{y}) \leq 0, \quad \exists \boldsymbol{x} \in X\} \tag{13}$$

For our hybrid MPC, we define the complicating variable $\boldsymbol{y}$ as the binary variable $\boldsymbol{\delta}$, the initial condition $\boldsymbol{x}_{in}$, and the parameter $\boldsymbol{\theta}$. The subproblem is:

$$\begin{aligned} v(\boldsymbol{x}_{in}, \boldsymbol{\theta}, \boldsymbol{\delta}) = \underset{\boldsymbol{x}\in X}{\text{minimize}} \quad & ||\boldsymbol{x} - \boldsymbol{x}_g||_{\boldsymbol{Q}}^2 \\ \text{s.t.} \quad & \boldsymbol{A}\boldsymbol{x} = \boldsymbol{b}(\boldsymbol{x}_{in}, \boldsymbol{\delta}) \\ & \boldsymbol{C}\boldsymbol{x} \leq \boldsymbol{d}(\boldsymbol{\theta}, \boldsymbol{\delta}) \end{aligned} \tag{14}$$

Given fixed $\boldsymbol{x}_{in}$, $\boldsymbol{\theta}$, $\boldsymbol{\delta}$, (14) is a quadratic programming (QP), with the feasible set of $\boldsymbol{\delta}$:

$$V(\boldsymbol{x}_{in}, \boldsymbol{\theta}) \coloneqq \{\boldsymbol{\delta} | \boldsymbol{A}\boldsymbol{x} = \boldsymbol{b}(\boldsymbol{x}_{in}, \boldsymbol{\delta}),\ \boldsymbol{C}\boldsymbol{x} \leq \boldsymbol{d}(\boldsymbol{\theta}, \boldsymbol{\delta}), \exists \boldsymbol{x} \in X\} \tag{15}$$

The master problem is:

$$\begin{aligned} \underset{\boldsymbol{\delta}}{\text{minimize}} \quad & v(\boldsymbol{x}_{in}, \boldsymbol{\theta}, \boldsymbol{\delta}) \\ \text{s.t.} \quad & \boldsymbol{\delta}_k \in \{0, 1\} \\ & \boldsymbol{\delta} \in V(\boldsymbol{x}_{in}, \boldsymbol{\theta}) \end{aligned} \tag{16}$$

Remark 2. *When nonlinear dynamics is linearized around a reference point that can be disturbed, random disturbances can cause a partial change of the system dynamics. In this case, part of $\boldsymbol{x}$ can also be placed as complicating variables. Some details are placed in Appendix I.*

The essential issue with solving (16) is that $v(\boldsymbol{x}_{in}, \boldsymbol{\theta}, \boldsymbol{\delta})$ and $V(\boldsymbol{x}_{in}, \boldsymbol{\theta})$ are only implicitly known through their definitions. Benders decomposition is a process that iteratively solves problem (11) and (12) to build approximations of v and V in the problem (11).

Given the advantage that the dual is invariant with respect to the complicating variables. We derive the dual problem of (14) for reference. Denote the dual problem by $\mathcal{D}(\boldsymbol{x}_{in}, \boldsymbol{\theta}, \boldsymbol{\delta})$, and its optimal cost by $d^*(\boldsymbol{x}_{in}, \boldsymbol{\theta}, \boldsymbol{\delta})$, we have:

$$\begin{aligned} &d^*(\boldsymbol{x}_{in}, \boldsymbol{\theta}, \boldsymbol{\delta}) = \\ &\underset{\boldsymbol{\nu},\ \boldsymbol{\lambda}}{\text{maximize}} \quad -\frac{1}{4}||\boldsymbol{A}^T\boldsymbol{\nu} + \boldsymbol{C}^T\boldsymbol{\lambda}||_{\boldsymbol{Q}^{-1}}^2 + \boldsymbol{x}_g^T(\boldsymbol{A}^T\boldsymbol{\nu} + \boldsymbol{C}^T\boldsymbol{\lambda}) \\ &\qquad\qquad - \boldsymbol{b}(\boldsymbol{x}_{in}, \boldsymbol{\delta})^T\boldsymbol{\nu} - \boldsymbol{d}(\boldsymbol{\theta}, \boldsymbol{\delta})^T\boldsymbol{\lambda} \\ &\qquad \text{s.t.} \quad \boldsymbol{\lambda} \geq \boldsymbol{0} \end{aligned} \tag{17}$$

where $\boldsymbol{\nu} \in \mathbb{R}^{(N+1)n_x}$, $\boldsymbol{\lambda} \in \mathbb{R}^{Nn_c}$ are the dual variables associated with $\boldsymbol{A}\boldsymbol{x} = \boldsymbol{b}(\boldsymbol{x}_{in}, \boldsymbol{\delta})$, $\boldsymbol{C}\boldsymbol{x} \leq \boldsymbol{d}(\boldsymbol{\theta}, \boldsymbol{\delta})$, respectively. The weak duality $d^*(\boldsymbol{x}_{in}, \boldsymbol{\theta}, \boldsymbol{\delta}) \leq v(\boldsymbol{x}_{in}, \boldsymbol{\theta}, \boldsymbol{\delta})$ holds even if the original subproblem is non-convex. Since our subproblem is convex and we assume there exists a stricly feasible solution (Slater's), strong duality is achieved: $d^*(\boldsymbol{x}_{in}, \boldsymbol{\theta}, \boldsymbol{\delta}) = v(\boldsymbol{x}_{in}, \boldsymbol{\theta}, \boldsymbol{\delta})$. Note that if $\boldsymbol{Q}_k$ are only positive semi-definite instead of positive definite as we have assumed, some extra care are required explained in Appendix II.

As the feasibility of (14) is independent of the objective function, (14) is feasible if

$$\begin{aligned} \underset{\boldsymbol{x}\in X}{\text{minimize}} \quad & \mathbf{0} \\ \text{s.t.} \quad & \boldsymbol{A}\boldsymbol{x} = \boldsymbol{b}(\boldsymbol{x}_{in}, \boldsymbol{\delta}) \\ & \boldsymbol{C}\boldsymbol{x} \leq \boldsymbol{d}(\boldsymbol{\theta}, \boldsymbol{\delta}) \end{aligned} \tag{18}$$

is feasible, which has the dual:

$$\begin{aligned} \underset{\boldsymbol{\nu},\ \boldsymbol{\lambda}}{\text{maximize}} \quad & -\boldsymbol{b}(\boldsymbol{x}_{in}, \boldsymbol{\delta})^T \boldsymbol{\nu} - \boldsymbol{d}(\boldsymbol{\theta}, \boldsymbol{\delta})^T \boldsymbol{\lambda} \\ \text{s.t.} \quad & \boldsymbol{A}^T \boldsymbol{\nu} + \boldsymbol{C}^T \boldsymbol{\lambda} = \mathbf{0} \\ & \boldsymbol{\lambda} \geq \mathbf{0} \end{aligned} \tag{19}$$

A. Feasibility cuts

If at iteration p, the subproblem is infeasible under the given $\boldsymbol{\delta}_p$, this $\boldsymbol{\delta}_p$ needs to be removed from the master problem. This can be achieved by adding a cutting plane. Since the problem (2) is linearly constrained, the Farkas certificates can be used to add feasibility cuts. They can be discovered by solving (18) with a dual simplex solver ([54], Section 6.5). The theorem of alternatives for (18) is:

Lemma 1. *Given $\boldsymbol{A} \in \mathbb{R}^{l\times n}$, $\boldsymbol{b} \in \mathbb{R}^l$, $\boldsymbol{C} \in \mathbb{R}^{m\times n}$, $\boldsymbol{d} \in \mathbb{R}^m$, exactly one of the following statements is true:*

1) *There exists an $\boldsymbol{x} \in \mathbb{R}^n$ that satisfies $\boldsymbol{A}\boldsymbol{x} = \boldsymbol{b}, \boldsymbol{C}\boldsymbol{x} \leq \boldsymbol{d}$.*
2) *There exist $\boldsymbol{y} \in \mathbb{R}^l$, $\boldsymbol{z} \in \mathbb{R}^m$ that satisfy $\boldsymbol{z} \geq \mathbf{0}$, $\boldsymbol{A}^T\boldsymbol{y} + \boldsymbol{C}^T\boldsymbol{z} = \mathbf{0}$, $\boldsymbol{b}^T\boldsymbol{y} + \boldsymbol{d}^T\boldsymbol{z} < 0$.*

Proof. This is a straightforward application of the Farkas' lemma (Theorem 4.6 in [54]). We provide a complete proof in Appendix III for readers who are unfamiliar with the topic. □

If (18) is infeasible for $\boldsymbol{\delta}_p$. Then we can add a cutting plane to the master problem to remove a set of $\boldsymbol{\delta}$'s including $\boldsymbol{\delta}_p$. Farkas lemma guarantees the existence of $\widetilde{\boldsymbol{\nu}}_p \in \mathbb{R}^{(N+1)n_x}$, $\widetilde{\boldsymbol{\lambda}}_p \in \mathbb{R}^{Nn_c}$ such that:

$$\begin{aligned} & \widetilde{\boldsymbol{\lambda}}_p \geq \mathbf{0} \\ & \boldsymbol{A}^T\widetilde{\boldsymbol{\nu}}_p + \boldsymbol{C}^T\widetilde{\boldsymbol{\lambda}}_p = \mathbf{0} \\ & \boldsymbol{b}(\boldsymbol{x}_{in}, \boldsymbol{\delta}_p)^T\widetilde{\boldsymbol{\nu}}_p + \boldsymbol{d}(\boldsymbol{\theta}, \boldsymbol{\delta}_p)^T\widetilde{\boldsymbol{\lambda}}_p < 0 \end{aligned} \tag{20}$$

To prevent the master problem from giving this $\boldsymbol{\delta}_p$ again, a constraint to defeat the Farkas infeasible proof is added to the master problem:

$$\boldsymbol{b}(\boldsymbol{x}_{in}, \boldsymbol{\delta})^T\widetilde{\boldsymbol{\nu}}_p + \boldsymbol{d}(\boldsymbol{\theta}, \boldsymbol{\delta})^T\widetilde{\boldsymbol{\lambda}}_p \geq 0 \tag{21}$$

This cutting plane will not remove any $\boldsymbol{\delta}$ feasible for the subproblem. We state this as a lemma.

Lemma 2. *For given $\boldsymbol{x}_{in}$ and $\boldsymbol{\theta}$, any $\boldsymbol{\delta}$ that contradicts (21) proves infeasibility for (18).*

Proof. As $\widetilde{\boldsymbol{\nu}}_p$, $\widetilde{\boldsymbol{\lambda}}_p$ discovered by the dual simplex solver satisfy the first two conditions of (20), they are feasible for the dual problem (19). Let $a \in \mathbb{R}^+$ be an arbitrary positive value, $(a\widetilde{\boldsymbol{\nu}}_p, a\widetilde{\boldsymbol{\lambda}}_p)$ are also feasible for (19). Let $\boldsymbol{\delta}$ be any value that contradicts (21), we have $-a\widetilde{\boldsymbol{\nu}}_p^T\boldsymbol{b}(\boldsymbol{x}_{in}, \boldsymbol{\delta}) - a\widetilde{\boldsymbol{\lambda}}_p^T\boldsymbol{d}(\boldsymbol{\theta}, \boldsymbol{\delta}) \to +\infty$ as $a \to +\infty$, hence the dual problem is unbounded which proves that the primal problem (18) is infeasible (from Corollary 4.1 of [54]). □

It can be easily verified that the dual feasible set of (19) is a pointed cone. Therefore, we can guarantee feasibility by enumerating all non-equivalent (one is a positive scalar multiple of the other) extreme rays.

Since hybrid MPC needs to be solved fast online, it is important to maximize the usage of computations so the number of iteration to find a feasible solution is reduced. Many previous works added one feasibility cut each iteration. Some previous works [46], [55], [56] propose adding multiple cutting planes each iteration, or re-formulate the problem such that stronger cuts can be generated. However, the subproblem structure has not been explored by those papers. We propose an innovative technique to add multiple feasibility cuts to the master problem via subproblem recursive structure. The online computation time prevents us to solve any additional optimization problems (even convex ones), but those cutting planes can be retrieved without any additional computation given the planes we already have. Define $\widetilde{\boldsymbol{\nu}}_p^m$, $\widetilde{\boldsymbol{\lambda}}_p^m$, $m = 1, ..., N-1$ such that:

$$\begin{aligned} \widetilde{\boldsymbol{\nu}}_p^m[k] &= \begin{cases} \widetilde{\boldsymbol{\nu}}_p[k+m] & \forall k+m \leq N \\ \mathbf{0} & \forall k+m > N \end{cases} \\ \widetilde{\boldsymbol{\lambda}}_p^m[k] &= \begin{cases} \widetilde{\boldsymbol{\lambda}}_p[k+m] & \forall k+m \leq N-1 \\ \mathbf{0} & \forall k+m > N-1 \end{cases} \end{aligned} \tag{22}$$

For each m, we add a shifted cutting planes:

$$\boldsymbol{b}(\boldsymbol{x}_{in}, \boldsymbol{\delta})^T\widetilde{\boldsymbol{\nu}}_p^m + \boldsymbol{d}(\boldsymbol{\theta}, \boldsymbol{\delta})^T\widetilde{\boldsymbol{\lambda}}_p^m \geq 0, \quad m = 1, ..., M_p \tag{23}$$

We can deem $\widetilde{\boldsymbol{\nu}}_p^0 \triangleq \widetilde{\boldsymbol{\nu}}_p$, $\widetilde{\boldsymbol{\lambda}}_p^0 \triangleq \widetilde{\boldsymbol{\lambda}}_p$. M_p represents the maximal shifting amount. As the original $\widetilde{\boldsymbol{\nu}}_p$ and $\widetilde{\boldsymbol{\lambda}}_p$ do not need to have all non-zero entries, the shifting can stop at $\widetilde{\boldsymbol{\nu}}_p[1] = \mathbf{0}$ and $\widetilde{\boldsymbol{\lambda}}_p[0] = \mathbf{0}$. The maximal value of M_p should be $N-1$.

The addition of cuts (23) reduces the cold-start time. Intuitively, the non-zero terms in the Farkas certificate provides a set of constraints that conflict with each other causing infeasibility. While this may happen some time in the future e.g. the mode sequence tries to make an infeasible jump at time k, it is also informative at time $0, ..., k-1$. By shifting the Farkas proof back in time, we propagate failure modes backwards to maximize its usage.

Similar to $\widetilde{\boldsymbol{\nu}}_p$ and $\widetilde{\boldsymbol{\lambda}}_p$, we present:

Lemma 3. *$\widetilde{\boldsymbol{\nu}}_p^m$, $\widetilde{\boldsymbol{\lambda}}_p^m$ are extreme rays for any m.*

Proof. We can verify that $\forall m$, $\widetilde{\boldsymbol{\nu}}_p^m$, $\widetilde{\boldsymbol{\lambda}}_p^m$ are dual feasible given $\widetilde{\boldsymbol{\nu}}_p$, $\widetilde{\boldsymbol{\lambda}}_p$ are dual feasible by plugging them into (19). Furthermore, $\widetilde{\boldsymbol{\nu}}_p^m$, $\widetilde{\boldsymbol{\lambda}}_p^m$ are rays since any positive scaling of them are still dual feasible. By shifting, all equality constraints remains active. Compared to the original inequality constraints, $\widetilde{\boldsymbol{\lambda}}_p[0] \geq \mathbf{0}$ is removed and $\widetilde{\boldsymbol{\lambda}}_p[N-1] = \mathbf{0}$ is appended at the end. Since $\widetilde{\boldsymbol{\lambda}}_p[N-1] = \mathbf{0}$ are all active for $\boldsymbol{\lambda} \geq \mathbf{0}$, the number of linearly independent constraints

at $(\widetilde{\boldsymbol{\nu}}_p^m, \widetilde{\boldsymbol{\lambda}}_p^m)$ does not decrease. The conclusion follows by definition 4.2 of [54]. □

As a simple extension of Lemma 2, we present:

Corollary 3.1. *Any $\boldsymbol{\delta}$ that contradicts (23) proves infeasibility for (18) with given $\boldsymbol{x}_{in}$ and $\boldsymbol{\theta}$.*

Till this point, we have used $\boldsymbol{b}$ and $\boldsymbol{d}$, indicating that the arguments on feasibility cuts above are independent of the internal structures of $\boldsymbol{b}$ and $\boldsymbol{d}$ as long as they are constants given $(\boldsymbol{x}_{in}, \boldsymbol{\theta}, \boldsymbol{\delta})$. We now write out the specific structures for feasibility cuts given (5) and (7). Let:

$$\widetilde{\boldsymbol{\Lambda}}_p^m = \begin{bmatrix} \widetilde{\boldsymbol{\nu}}_p^m[0]^T & \widetilde{\boldsymbol{\lambda}}_p^m[0]^T & \cdots & \widetilde{\boldsymbol{\lambda}}_p^m[N-1]^T \end{bmatrix}^T \in \mathbb{R}^{n_x+Nn_c} \tag{24}$$

$$\widetilde{\boldsymbol{\mathcal{V}}}_p^m = \begin{bmatrix} \widetilde{\boldsymbol{\mathcal{V}}}_p^m[0]^T & \cdots & \widetilde{\boldsymbol{\mathcal{V}}}_p^m[N-1]^T \end{bmatrix}^T \in \mathbb{R}^{Nn_\delta} \tag{25}$$

$$\widetilde{\boldsymbol{\mathcal{V}}}_p^m[k] = \boldsymbol{G}^T \widetilde{\boldsymbol{\nu}}_p^m[k+1] - \boldsymbol{H}_3^T \widetilde{\boldsymbol{\lambda}}_p^m[k] \tag{26}$$

The cuts (21) and (23) can be written together as:

$$\widetilde{\boldsymbol{\Lambda}}_p^{mT} \boldsymbol{\Theta} + \widetilde{\boldsymbol{\mathcal{V}}}_p^{mT} \boldsymbol{\delta} \geq 0, \quad m = 0, 1, ..., M_p \tag{27}$$

It is interesting to realize that from an infeasible subproblem with one $\boldsymbol{\delta}$, we construct a plane that may remove a set of infeasible $\boldsymbol{\delta}$'s. This contributes to the efficacy of Benders decomposition as it takes usage of infeasible samples which are usually thrown away by the methods that learn binary solutions offline [13], [20], [27].

B. Optimality cuts

If at iteration q, the sub-problem is solved to optimal under given $(\boldsymbol{x}_{in,q}, \boldsymbol{\theta}_q, \boldsymbol{\delta}_q)$, and the QP solver returns dual variables $(\boldsymbol{\nu}_q^*, \boldsymbol{\lambda}_q^*)$ at optimum, we want to add a cutting plane as a lower bound that approaches $v(\boldsymbol{x}_{in}, \boldsymbol{\theta}, \boldsymbol{\delta})$ from below. This can be realized through duality theory. Let $v_q = v(\boldsymbol{x}_{in,q}, \boldsymbol{\theta}_q, \boldsymbol{\delta}_q)$. Define:

$$C_q = v_q + \boldsymbol{\nu}_q^{*T} \boldsymbol{b}(\boldsymbol{x}_{in,q}, \boldsymbol{\delta}_q) + \boldsymbol{\lambda}_q^{*T} \boldsymbol{d}(\boldsymbol{\theta}_q, \boldsymbol{\delta}_q) \tag{28}$$

We state that for any $(\boldsymbol{x}_{in}, \boldsymbol{\theta}, \boldsymbol{\delta})$, we have:

$$v(\boldsymbol{x}_{in}, \boldsymbol{\theta}, \boldsymbol{\delta}) \geq C_q - \boldsymbol{\nu}_q^{*T} \boldsymbol{b}(\boldsymbol{x}_{in}, \boldsymbol{\delta}) - \boldsymbol{\lambda}_q^{*T} \boldsymbol{d}(\boldsymbol{\theta}, \boldsymbol{\delta}) \tag{29}$$

This is a result that $(\boldsymbol{\nu}_q^*, \boldsymbol{\lambda}_q^*)$ is a feasible solution of $\mathcal{D}(\boldsymbol{x}_{in}, \boldsymbol{\theta}, \boldsymbol{\delta})$, and $-\frac{1}{4}||\boldsymbol{A}^T\boldsymbol{\nu}_q^* + \boldsymbol{C}^T\boldsymbol{\lambda}_q^*||^2_{\boldsymbol{Q}^{-1}} + \boldsymbol{x}_g^T(\boldsymbol{A}^T\boldsymbol{\nu}_q^* + \boldsymbol{C}^T\boldsymbol{\lambda}_q^*) = v_q + \boldsymbol{\nu}_q^{*T}\boldsymbol{b}(\boldsymbol{x}_{in,q}, \boldsymbol{\delta}_q) + \boldsymbol{\lambda}_q^{*T}\boldsymbol{d}(\boldsymbol{\theta}_q, \boldsymbol{\delta}_q)$ due to strong duality at $(\boldsymbol{x}_{in,q}, \boldsymbol{\theta}_q, \boldsymbol{\delta}_q)$.

We add (29) to the master problem as a lower bound for general $\boldsymbol{\delta}$. Since this is a lower bound, it will keep searching for potentially better solutions. This procedure continues until the lower bound is tight at some iteration when no potentially better solution can be found, and a global optimal $\boldsymbol{\delta}_q$ is returned. As $\boldsymbol{x}_{in}$ and $\boldsymbol{\theta}$ take the same position as $\boldsymbol{\delta}$ in $\mathcal{L}$, the lower bound also applies when $\boldsymbol{x}_{in}$ and $\boldsymbol{\theta}$ are updated. This will be used to construct warm-starts for hybrid MPC.

Remark 3. *Since problem (17) minimizes $||\boldsymbol{A}^T\boldsymbol{\nu} + \boldsymbol{C}^T\boldsymbol{\lambda}||^2_{\boldsymbol{Q}^{-1}}$, $(\boldsymbol{\nu}^*, \boldsymbol{\lambda}^*)$ should make $\boldsymbol{A}^T\boldsymbol{\nu} + \boldsymbol{C}^T\boldsymbol{\lambda}$ small (if the cost is linear, $(\boldsymbol{\nu}^*, \boldsymbol{\lambda}^*)$ are extreme points of the cone $\boldsymbol{A}^T\boldsymbol{\nu} + \boldsymbol{C}^T\boldsymbol{\lambda} = \boldsymbol{0}$). Therefore, dual solutions depends on linear dynamics. Assume the parameters follow some distribution $(\boldsymbol{\Theta}, \boldsymbol{\delta}) \sim \mathcal{G}(\boldsymbol{\Theta}, \boldsymbol{\delta})$, By enumerating dual solutions, the master problem learns a distribution of $(\boldsymbol{\nu}^*, \boldsymbol{\lambda}^*)$ to construct the cost map, under the linear dynamics unknown to the master problem. On the other hand, the general cost map conditioned on $\boldsymbol{A}$, $\boldsymbol{C}$ could also be learned offline and used to cold-start the GBD algorithm.*

Similar to feasibility cuts, we have used $\boldsymbol{b}$ and $\boldsymbol{d}$, indicating that the arguments on optimality cuts above are independent of their internal structures. We now write out the specific structures for optimality cuts. Let:

$$\boldsymbol{\Lambda}_q^* = \begin{bmatrix} \boldsymbol{\nu}_q^*[0]^T & \boldsymbol{\lambda}_q^*[0]^T & \cdots & \boldsymbol{\lambda}_q^*[N-1]^T \end{bmatrix}^T \in \mathbb{R}^{n_x+Nn_c} \tag{30}$$

$$\boldsymbol{\mathcal{V}}_q^* = \begin{bmatrix} \boldsymbol{\mathcal{V}}_q^*[0]^T & \cdots & \boldsymbol{\mathcal{V}}_q^*[N-1]^T \end{bmatrix}^T \in \mathbb{R}^{Nn_\delta} \tag{31}$$

$$\boldsymbol{\mathcal{V}}_q^*[k] = \boldsymbol{G}^T \boldsymbol{\nu}_q^*[k+1] - \boldsymbol{H}_3^T \boldsymbol{\lambda}_q^*[k] \tag{32}$$

The cut (29) can be written as:

$$v(\boldsymbol{\Theta}, \boldsymbol{\delta}) \geq C_q - \boldsymbol{\Lambda}_q^{*T} \boldsymbol{\Theta} - \boldsymbol{\mathcal{V}}_q^{*T} \boldsymbol{\delta} \tag{33}$$

$$C_q = v_q + \boldsymbol{\Lambda}_q^{*T} \boldsymbol{\Theta}_q + \boldsymbol{\mathcal{V}}_q^{*T} \boldsymbol{\delta}_q \tag{34}$$

C. The Benders master problem

As the algorithm iterates, an index set is formed: $\mathcal{I} \triangleq \{1, 2, ..., \text{current iteration}\}$. Among this set, we define sub-index set $\{p\} \subseteq \mathcal{I}$ to be indices of infeasible subproblem, and another sub-index set $\{q\} \subseteq \mathcal{I}$ to be indices of feasible subproblem. Note that $\{p\} \cup \{q\} = \mathcal{I}$ and $\{p\} \cap \{q\} = \emptyset$. The final form of the master problem (16) is:

$$\begin{aligned} \underset{\boldsymbol{\delta}}{\text{minimize}} \quad & z_0 \\ \text{s.t.} \quad & \boldsymbol{\delta}[k] \in \{0,1\}^{n_\delta} \\ & \widetilde{\boldsymbol{\Lambda}}_p^{mT} \boldsymbol{\Theta}_p + \widetilde{\boldsymbol{\mathcal{V}}}_p^{mT} \boldsymbol{\delta} \geq 0, \quad m = 0, 1, ..., M_p, \quad \forall p \in \{p\} \\ & z_0 \geq C_q - \boldsymbol{\Lambda}_q^{*T} \boldsymbol{\Theta}_q - \boldsymbol{\mathcal{V}}_q^{*T} \boldsymbol{\delta}, \quad \forall q \in \{q\} \end{aligned} \tag{35}$$

where z_0 is an epigraph variable such that $z_0 \geq v(\boldsymbol{x}_{in}, \boldsymbol{\theta}, \boldsymbol{\delta}_q)\ \forall q$ finds the smallest value of optimality cuts. This is an MIP problem that contains $2N$ binary variables and one continuous variable. As the algorithm proceeds, constraints will be added to the master problem. In section VI, we propose a fast greedy algorithm that leverages on the sparsity of the feasibility cuts to solve this problem. On the other hand, this problem can also be solved using commercialized MIP solvers. It oftentimes can be resolved at the presolve stage for our tested problems.

D. Upper and lower objective bounds

Benders decomposition is an iterative procedure that adds feasibility cuts and optimality cuts to improve the approximation of v and V in the master problem. Since the optimality cuts are lower bounds of the actual cost v, the master problem will be "too optimistic" about the subproblem, proposing $\boldsymbol{\delta}$ that is oftentimes infeasible, or with an optimal cost cannot be reached by the subproblem. As more cuts are added, the lower bound increases, describing the actual costs better. If the MIP solver finds the global optimal value of the master problem at each iteration, the lower bound does not decrease as the algorithm iterates.

On the other hand, the best subproblem cost till the current iteration provides a upper bound of the global optimal cost. Since the stored cuts in the master problem underestimate the actual subproblem cost, the subproblem costs may even increase as the algorithm iterates. The upper bound is introduced to keep track of the best cost.

As the algorithm proceeds, the lower bound and upper bound will approach each other. Eventually, they converge to each other and the algorithm terminates (a proof of convergence can be found in [12]). We introduce the g_a for the termination condition. For fair comparison, we use the same definition as Gurobi [57]:

$$g_a = |z_P - z_D|/|z_P| \tag{36}$$

where z_P is the primal bound, or upper bound of the global optimal cost, and z_D is the dual bound, or the lower bound of the cost. When g_a is smaller than a predefined threshold G_a, the inner loop algorithm terminates with an optimal $\boldsymbol{\delta}^*$ and control signal $\boldsymbol{u}^*$. Define I_{max} as the maximal number of GBD iterations. The non-warm-started GBD is presented in Algorithm 1.

Algorithm 1: GBD

Input: G_a, I_{max}, feas. cuts $= \{\}$, opt. cuts $= \{\}$
Intialization $LB \coloneqq -\infty$, $UB \coloneqq \infty$, iteration $i \coloneqq 0$
while $|UB - LB|/|UB| \geq G_a$ **do**
  Solve master problem (35) with current feas. cuts and opt. cuts, get $\boldsymbol{\delta}$ and cost m_i^*
  $LB \coloneqq m_i^*$
  if $g_a \leq G_a$ *or* $i \geq I_{max}$ **then**
    Break
  Solve subQP (14) with $\boldsymbol{\delta}$
  if *Feasible* **then**
    Solver returns cost v_i, dual $\boldsymbol{\nu}_i^*$, $\boldsymbol{\lambda}_i^*$
    if v_i<*UB* **then**
      Let $UB \coloneqq v_i$, $\boldsymbol{u}^* \coloneqq \boldsymbol{u}$
    Add constraint (33) to opt. cuts
  else Infeasible
    Solve (18) with dual simplex, solver returns Farkas proof $\widetilde{\boldsymbol{\nu}}_i$, $\widetilde{\boldsymbol{\lambda}}_i$
    Add constraints (27) to feas. cuts
  $i \coloneqq i + 1$
return $\boldsymbol{u}^*$, *feas. cuts, opt. cuts*

V. Continual learning and warm-start

The idea behind the Benders decomposition for linear programming subproblems [33] is to enumerate extreme rays and extreme points in the dual, and construct cuts based on them. If all extreme rays and extreme points are enumerated, the master problem has the complete cost map $v(\boldsymbol{\Theta}, \boldsymbol{\delta})$ to search for optimal binary solutions, through solving an MIP. For QP subproblems, the optimal solutions are not necessarily extreme points, but not far from them due to the minimization of $||\boldsymbol{A}^T\boldsymbol{\nu} + \boldsymbol{C}^T\boldsymbol{\lambda}||$. As long as this norm is bounded and all feasibility cuts are added, the dual solutions $(\boldsymbol{\nu}^*, \boldsymbol{\lambda}^*)$ come from a bounded (hence totally bounded) region which can be finitely covered by open balls $B_\epsilon(\boldsymbol{\nu}^*, \boldsymbol{\lambda}^*)$. We also recall that the number of non-equivalent extreme rays for a polyhedron is finite ([54], Section 4.8). This means that in theory, $v(\boldsymbol{\Theta}, \boldsymbol{\delta})$ and $V(\boldsymbol{\Theta})$ can be completely constructed offline with finite number of Farkas proofs and optimal duals. However, the number of Farkas proofs and optimal duals is astronomical, hence the time and storage requirements will simply explode. GBD avoids this by generating Farkas proofs and optimal duals in the course of computation as they are needed.

In this paper, we extend this idea to continual learning inside a dynamic environment represented by $\boldsymbol{\Theta}$ shifting online. Intuitively, Farkas proofs represent the way the system fails, and optimal dual variables represent the best way to distribute the constraint efforts. Despite $\boldsymbol{\Theta}$ being pushed forward along the trajectory, if the dual solutions do not drastically vary, the algorithm can quickly enumerate them in the first few problem samples, and the rest problems can be solved with much fewer trials. To prevent overloading the master problem with cuts, we set up a finite buffer that adds new cuts and throws out irrelevant ones. A larger buffer provides extra robustness against larger disturbances. This approach can be more data efficient than learning methods that consumes a large set of solved problems offline, trying to construct the parametric $\boldsymbol{\Theta} \to \boldsymbol{\delta}$ mapping, such as [3], [13], [25], [27], [58]. In fact, it is found that a small number of dual solutions can already generate good warm-starts for the $\boldsymbol{\Theta}$ trajectory.

A. Warm-starting using existing cuts

As MPC proceeds online, the problem (2) needs to be constantly resolved with different $\boldsymbol{\Theta}$. Since $\boldsymbol{\Theta}$ take the same position in the subproblem (14) as $\boldsymbol{\delta}$, all the optimality cuts (33) that construct lower bounds for $\boldsymbol{\delta}$ are also valid lower bounds for $\boldsymbol{\Theta}$. In addition, the feasibility cuts (21) can also be used for new $\boldsymbol{\Theta}$ as $\widetilde{\boldsymbol{\nu}}_p$, $\widetilde{\boldsymbol{\lambda}}_p$ are independent of $\boldsymbol{\Theta}$. Assume we have feasible and optimality cuts as listed in (35). When new $\boldsymbol{\Theta}'$ come in, we update the cutting planes (27) and (33) to:

$$\widetilde{\boldsymbol{\Lambda}}_p^{mT}\boldsymbol{\Theta}' + \widetilde{\boldsymbol{\mathcal{V}}}_p^{mT}\boldsymbol{\delta} \geq 0, \quad m = 0, 1, ..., M_p, \quad \forall p \in \{p\} \tag{37}$$

$$z_0 \geq C_q - \mathbf{\Lambda}_q^{*T}\mathbf{\Theta}' - \boldsymbol{\mathcal{V}}_q^{*T}\boldsymbol{\delta}, \quad \forall q \in \{q\} \tag{38}$$

If we let $\Delta\mathbf{\Theta}_i = \mathbf{\Theta}' - \mathbf{\Theta}_i$, another way to look at this updating is we add a correction term $\widetilde{\mathbf{\Lambda}}_p^{mT}\Delta\mathbf{\Theta}_p$ at the left hand side of (27), and add a correction term $-\mathbf{\Lambda}_q^{*T}\Delta\mathbf{\Theta}_q$ at the right hand side of (33).

With this simple trick, we use previously enumerated cuts to build warm-starts for $\mathbf{\Theta}'$. This $\mathbf{\Theta}'$ is then fixed, and Algorithm 1 runs again, but with non-empty feasibility cuts and optimality cuts that allows the master problem to provide good $\boldsymbol{\delta}$ in the beginning.

Similar to Lemma 2, we present:

Corollary 3.2. *For given $\mathbf{\Theta}'$, any $\boldsymbol{\delta}$ that contradicts (37) proves infeasibility for (18). In addition:*

$$v(\mathbf{\Theta}', \boldsymbol{\delta}) \geq C_q - \mathbf{\Lambda}_q^{*T}\mathbf{\Theta}' - \boldsymbol{\mathcal{V}}_q^{*T}\boldsymbol{\delta}$$

Proof. This is a simple result from Lemma 2 given $\widetilde{\boldsymbol{\nu}}_p$ and $\widetilde{\boldsymbol{\lambda}}_p$ are independent of $\boldsymbol{x}_{in}$ and $\boldsymbol{\theta}$, and that $\mathbf{\Theta}$ and $\boldsymbol{\delta}$ take the same position in (29). □

For a more clear explanation, let the set of enumerated dual variables $\widetilde{\mathcal{F}} \triangleq \{(\widetilde{\mathbf{\Lambda}}_p^m, \widetilde{\boldsymbol{\mathcal{V}}}_p^m) |\ p \in \{p\}, \forall m\}$, $\mathcal{O}^* \triangleq \{(\mathbf{\Lambda}_q^*, \boldsymbol{\mathcal{V}}_q^*, C_q) |\ q \in \{q\}\}$. On top of that, the cuts are composed of dual solutions and $\mathbf{\Theta}$. The set of feasibility cuts $\mathcal{T}_f(\mathbf{\Theta}) \triangleq \widetilde{\mathcal{F}} \times \mathbf{\Theta}$. The set of optimality cuts $\mathcal{T}_o(\mathbf{\Theta}) \triangleq \mathcal{O}^* \times \mathbf{\Theta}$.

B. Tightness of lower bounds

Since optimality cuts provide lower bounds for $v(\mathbf{\Theta}, \boldsymbol{\delta})$, we want to investigate the gap between v and the lower bounds. An assumption is made to quantify the change of v:

Assumption 1. *(Lipschitz condition) The optimal cost function $v(\mathbf{\Theta}, \boldsymbol{\delta})$ satisfies:*

$$|v(\mathbf{\Theta}', \boldsymbol{\delta}') - v(\mathbf{\Theta}, \boldsymbol{\delta})| \leq L||\Delta\mathbf{\Theta}||_2 + L_\delta||\Delta\boldsymbol{\delta}||_2 \tag{39}$$

This Lipschitz condition bounds the gap:

Corollary 3.3. *For one feasibility cut $q \in \{q\}$, define the gap as $g_q(\mathbf{\Theta}, \boldsymbol{\delta}) = v(\mathbf{\Theta}, \boldsymbol{\delta}) - z_0(\mathbf{\Theta}, \boldsymbol{\delta})$, where z_0 is the optimality cut evaluated at $(\mathbf{\Theta}, \boldsymbol{\delta})$ (with a slight abuse of notation):*

$$z_0 = C_q - \mathbf{\Lambda}_q^{*T}\mathbf{\Theta} - \boldsymbol{\mathcal{V}}_q^{*T}\boldsymbol{\delta} \tag{40}$$

For any feasible $\boldsymbol{\delta}$ under $\mathbf{\Theta}$, we have:

$$\begin{aligned} 0 \leq g_q(\mathbf{\Theta}, \boldsymbol{\delta}) \leq L||\Delta\mathbf{\Theta}_q||_2 + \boldsymbol{\mathcal{V}}_q^{*T}\Delta\mathbf{\Theta}_q \\ + L_\delta\sqrt{(N+1)n_\delta} + ||\boldsymbol{\mathcal{V}}_q^*||_1 \end{aligned} \tag{41}$$

Proof. Since the optimality cuts provide lower bounds for $v(\mathbf{\Theta}, \boldsymbol{\delta})$, $g(\mathbf{\Theta}, \boldsymbol{\delta}) \geq 0$. In fact, g can be arbitrarily close to 0 since we do not know the curvature of v.

To prove the second inequality, we note that $z_0(\mathbf{\Theta}_q, \boldsymbol{\delta}_q) = v_q$ due to strong duality, hence $C_q = v_q + \mathbf{\Lambda}_q^{*T}\mathbf{\Theta}_q + \boldsymbol{\mathcal{V}}_q^{*T}\boldsymbol{\delta}_q$. Therefore:

$$z_0(\mathbf{\Theta}, \boldsymbol{\delta}) = v_q - \mathbf{\Lambda}_q^{*T}\Delta\mathbf{\Theta}_q - \boldsymbol{\mathcal{V}}_q^{*T}(\boldsymbol{\delta} - \boldsymbol{\delta}_q) \tag{42}$$

In addition, $v(\mathbf{\Theta}, \boldsymbol{\delta}) \leq v_q + L||\Delta\mathbf{\Theta}_q||_2 + L_\delta||\boldsymbol{\delta} - \boldsymbol{\delta}_q||_2$ via Lipschitz condition, hence we have:

$$\begin{aligned} &g_q(\mathbf{\Theta}, \boldsymbol{\delta}) = v(\mathbf{\Theta}, \boldsymbol{\delta}) - z_0(\mathbf{\Theta}, \boldsymbol{\delta}) \\ &\leq L||\Delta\mathbf{\Theta}_q||_2 + \mathbf{\Lambda}_q^{*T}\Delta\mathbf{\Theta}_q + L_\delta||\boldsymbol{\delta} - \boldsymbol{\delta}_q||_2 + \boldsymbol{\mathcal{V}}_q^{*T}(\boldsymbol{\delta} - \boldsymbol{\delta}_q) \\ &\leq L||\Delta\mathbf{\Theta}_q||_2 + \mathbf{\Lambda}_q^{*T}\Delta\mathbf{\Theta}_q + L_\delta\sqrt{(N+1)n_\delta} + ||\boldsymbol{\mathcal{V}}_q^*||_1 \end{aligned} \tag{43}$$

The last step is due to that $\boldsymbol{\delta}$ is a binary variable of length $(N+1)n_\delta$. □

The meaning of the second inequality of (41) is clear. The $L||\Delta\mathbf{\Theta}_q||_2$ term is due to the change of $v(\mathbf{\Theta}, \boldsymbol{\delta})$ given $\Delta\mathbf{\Theta}$. The $\boldsymbol{\mathcal{V}}_q^{*T}\Delta\mathbf{\Theta}_q$ term is due to the change of optimality cuts along $\mathbf{\Theta}$ direction. The rest two terms are due to the change of optimal binary solutions. Because this is a parametric MIQP, we have two sets of parameters for subQPs: $\mathbf{\Theta}$ assigned by the environment, and $\boldsymbol{\delta}^*$ by solving master problems. Changes of each parameter can result in looser lower bounds.

C. Quadratic programming subproblems

In general, the Lipschitz constant from Assumption 1 is difficult to retrieve. However, when the subproblem is simpler, the Lipschitz constants can be computed under certain conditions. In this paper, the subproblems are QPs. Multi-parametric QPs have been studied by [24], showing that $V(\mathbf{\Theta})$ is convex, and $v(\mathbf{\Theta}, \boldsymbol{\delta})$ is continuous, convex, and piecewise quadratic. In this section, we use these results to compute Lipschitz constant within the same critical region (the active set remains unchanged at optimum), where the cost is continuous and quadratic. We state this as a lemma:

Lemma 4. *Given two parameters $\mathbf{\Theta}_1$ and $\mathbf{\Theta}_2$ and their optimal binary solutions $\boldsymbol{\delta}_1^*$ and $\boldsymbol{\delta}_2^*$. Assume the active inequality constraints in (14) do not change from $(\mathbf{\Theta}_1, \boldsymbol{\delta}_1^*)$ to $(\mathbf{\Theta}_2, \boldsymbol{\delta}_2^*)$. We have:*

$$\begin{aligned} &|v(\mathbf{\Theta}_2, \boldsymbol{\delta}_2^*) - v(\mathbf{\Theta}_1, \boldsymbol{\delta}_1^*)| \leq \\ &\qquad 2||\begin{bmatrix}\mathbf{\Theta}_0^T & \boldsymbol{\delta}_0^T\end{bmatrix}\boldsymbol{\mathcal{H}}||_2||\begin{bmatrix}\Delta\mathbf{\Theta}^T & \Delta\boldsymbol{\delta}^{*T}\end{bmatrix}||_2 \end{aligned} \tag{44}$$

where $\begin{bmatrix}\mathbf{\Theta}_0^T & \boldsymbol{\delta}_0^T\end{bmatrix}$ is a point on the line segment between $\begin{bmatrix}\mathbf{\Theta}_1^T & \boldsymbol{\delta}_1^{*T}\end{bmatrix}$ and $\begin{bmatrix}\mathbf{\Theta}_2^T & \boldsymbol{\delta}_2^{*T}\end{bmatrix}$. $\boldsymbol{\mathcal{H}}$ is defined through (64).

Proof. See Appendix IV. □

Remark 4. *Since we have a piecewise quadratic model of the objective values, instead of using linear cuts, we can also fit a piecewise quadratic function and use it to under-estimate $v(\boldsymbol{\theta}, \boldsymbol{\delta})$ in the master problem.*

Through triangular inequality, $L||\begin{bmatrix}\Delta\mathbf{\Theta}^T & \Delta\boldsymbol{\delta}^{*T}\end{bmatrix}||_2 \leq L||\Delta\mathbf{\Theta}||_2 + L||\Delta\boldsymbol{\delta}||_2$, thus a simple choice is $L = L_\delta = 2||\begin{bmatrix}\mathbf{\Theta}_0^T & \boldsymbol{\delta}_0^T\end{bmatrix}\boldsymbol{\mathcal{H}}||_2$.

However, the active set can change due to change of $(\mathbf{\Theta}, \boldsymbol{\delta}^*)$. In general, it is difficult to predict the active set for the optimal solution, hence the Lipschitz constant is difficult to compute. Without it, we cannot bound g_q, and the performance of optimality cuts may deteriorate. Previous works such as [59] pre-computes any critical regions offline.

[60] re-computes search directions every time the candidate solution crosses the boundary of critical regions, following homotopy lines.

On the other hand, our algorithm constructs lower bounds from Benders cuts irrespective of the active sets. The candidate solutions in our algorithm do not follow the homotopy lines as [60] does, but can take large jumps, making it difficult to guarantee the performance of a single cut. If we have enough quantity of cuts with dual solutions that are not too close, at each $\boldsymbol{\Theta}$ on the trajectory there may be a few cuts having small g_q, meaning the collection of cuts captures the general trend of $v(\boldsymbol{\Theta}, \boldsymbol{\delta})$.

D. Cut storage

If the continual learning algorithm keeps storing cuts, its quantity can increase to where the master problem becomes very expensive to solve. In this section, we use a finite buffer to alleviate the challenge of scaling up, given that the current problem only needs a portion of all enumerated cuts. Let K_{feas} and K_{opt} be the maximal buffer sizes for feasibility and optimality cuts. Assuming the noise is moderate, hence $\boldsymbol{\Theta}$ does not vary significantly in time. The recent cuts will be deep for the current problem. If the buffer is full, the oldest cuts are removed when new cuts are stored. If the noise becomes larger and breaks the temporal relationship, one can use the cut depth as the metric and sort out the best cuts from a long term storage. Meanwhile, a better model to reduce the noise may be preferred.

When cuts are stored, only those with dual variables sufficiently far-away are stored to save space. Since feasibility cuts are homogeneous, we use angles to measure distance between Farkas proofs. Let α be the threshold of angle. When two Farkas proofs $(\widetilde{\boldsymbol{\nu}}_1, \widetilde{\boldsymbol{\lambda}}_1)$ and $(\widetilde{\boldsymbol{\nu}}_2, \widetilde{\boldsymbol{\lambda}}_2)$ has angle between then less than α, or $(\widetilde{\boldsymbol{\nu}}_1, \widetilde{\boldsymbol{\lambda}}_1) \in A_\alpha(\widetilde{\boldsymbol{\nu}}_2, \widetilde{\boldsymbol{\lambda}}_2)$, we only store one of them. On the other hand, the distances between optimal duals are quantified by Euclidean distance with a threshold ϵ. When two optimal dual variables $(\boldsymbol{\nu}_1^*, \boldsymbol{\lambda}_1^*)$ and $(\boldsymbol{\nu}_2^*, \boldsymbol{\lambda}_2^*)$ satisfy $(\boldsymbol{\nu}_1^*, \boldsymbol{\lambda}_1^*) \in B_\epsilon(\boldsymbol{\nu}_2^*, \boldsymbol{\lambda}_2^*)$, we only store one of them. This data storage is given by Algorithm 2.

Algorithm 2: Cut Storage

Input: $\widetilde{\mathcal{F}}$, $\mathcal{O}^*$, $(\widetilde{\boldsymbol{\nu}}_i, \widetilde{\boldsymbol{\lambda}}_i)$, $(\boldsymbol{\nu}_i^*, \boldsymbol{\lambda}_i^*)$, ϵ, α, K_{feas}, K_{opt}

if $(\widetilde{\boldsymbol{\nu}}_i, \widetilde{\boldsymbol{\lambda}}_i) \notin A_\alpha(\widetilde{\boldsymbol{\nu}}, \widetilde{\boldsymbol{\lambda}})\ \forall (\widetilde{\boldsymbol{\nu}}, \widetilde{\boldsymbol{\lambda}}) \in \widetilde{\mathcal{F}}$ **then**
  Append $(\widetilde{\boldsymbol{\nu}}_i, \widetilde{\boldsymbol{\lambda}}_i)$ to the end of $\widetilde{\mathcal{F}}$
  if $|\widetilde{\mathcal{F}}| > K_{feas}$ **then**
    Remove the first element in $\widetilde{\mathcal{F}}$
if $(\boldsymbol{\nu}_i^*, \boldsymbol{\lambda}_i^*) \notin B_\epsilon(\boldsymbol{\nu}^*, \boldsymbol{\lambda}^*)\ \forall (\boldsymbol{\nu}^*, \boldsymbol{\lambda}^*) \in \mathcal{O}^*$ **then**
  Append $(\boldsymbol{\nu}_i^*, \boldsymbol{\lambda}_i^*)$ to the end of $\mathcal{O}^*$
  if $|\mathcal{O}^*| > K_{opt}$ **then**
    Remove the first element in $\mathcal{O}^*$
return $\widetilde{\mathcal{F}}$, $\mathcal{O}^*$

We note that the GBD iteration terminates when the upper cost bound and lower cost bound are close enough, which *proves* the optimality of the current $\boldsymbol{\delta}^*$. However, only the cuts till the iteration where control $\boldsymbol{\delta}^*$ is produced for the first time is necessary to reproduce $\boldsymbol{\delta}^*$ in the future problems. After this, the cuts are generated to prove optimality, which are not stored.

Finally, we present the outer MPC loop with continual learning and warm-start in Algorithm 3.

Algorithm 3: GBD MPC with continual learning

Input: ϵ, α, K_{feas}, K_{opt}, G_a, I_{max}
Intialization $\widetilde{\mathcal{F}} = \{\}$, $\mathcal{O}^* = \{\}$
Loop
  Get $\boldsymbol{\Theta}$ from state estimation
  Update $\boldsymbol{\Theta}$ in all cuts, or equivalently, generate $\mathcal{T}_f = \widetilde{\mathcal{F}} \times \boldsymbol{\Theta}$, $\mathcal{T}_o = \mathcal{O}^* \times \boldsymbol{\Theta}$
  $\boldsymbol{u}^*$, $\{(\widetilde{\boldsymbol{\nu}}_i, \widetilde{\boldsymbol{\lambda}}_i)\}$, $\{(\boldsymbol{\nu}_i^*, \boldsymbol{\lambda}_i^*)\}$ = GBD(G_a, I_{max}, $\mathcal{T}_f$, $\mathcal{T}_o$)
  Implement control $\boldsymbol{u}^*$
  $\widetilde{\mathcal{F}}$, $\mathcal{O}^*$ = Cut_Storage($\widetilde{\mathcal{F}}$, $\mathcal{O}^*$, $\{(\widetilde{\boldsymbol{\nu}}_i, \widetilde{\boldsymbol{\lambda}}_i)\}$, $\{(\boldsymbol{\nu}_i^*, \boldsymbol{\lambda}_i^*)\}$, ϵ, α, K_{feas}, K_{opt})

Remark 5. *In this paper, we store the cuts after the GBD converges. However, cut storage can also happen in-parallel with the GBD iterations under a different thread, as GBD generates cuts before convergence. This may further increase the solving speed.*

VI. Algorithm for Benders Master Problem

In this section, we present an efficient algorithm to solve the Benders master problem (35) leveraging on the sparsity of feasibility cuts. Since the master problem is an integer programming problem, its solving speed can be slow. Commercialized Branch and Bound solvers need to search $2^{Nn_\delta} = (2^{n_\delta})^N$ branches in the worst case, an exponential number with respect to the time horizon. For each branch, a convex subproblem needs to be solved. Therefore, the solving speed can be slow. Some previous works, such as [43], reported over 90% solving time on the master problem.

Several previous works [61]–[63] have analyzed or utilized sparsity of cuts to improve the computational performance for their MILP formulations. In particular, [63] connects the sparsity of cuts to the sparsity of constraint matrices. Our constraint matrices $\boldsymbol{A}$, $\boldsymbol{C}$ have sparse structure provided by the dynamic constraints, and the feasibility cuts are found to be sparse as they come from solving linear programs. The sparsity is further enforced by the shifted feasibility cuts. We propose a greedy search algorithm to solve (35). This algorithm is also inspired by the depth-first-search rounding algorithm that depends on depth-first search [64] to solve binary variables out of their tight convex relaxation.

We first write out the structure of (35). For each iteration p that the subproblem is infeasible, a number of feasibility cuts will be added to the master problem. Due to shifting, $\widetilde{\boldsymbol{\nu}}_p^m[k] = \boldsymbol{0}$, $\widetilde{\boldsymbol{\lambda}}_p^m[k] = \boldsymbol{0}$ for k from a certain time step till the end of time horizon. We organize the cuts such that if a cut

with certain p, m has $\widetilde{\boldsymbol{\nu}}_p^m[1] \neq \mathbf{0}$ or $\widetilde{\boldsymbol{\lambda}}_p^m[0] \neq \mathbf{0}$, but $\widetilde{\boldsymbol{\nu}}_p^m[k] = \mathbf{0}$ for $k = 2, ..., N$, $\widetilde{\boldsymbol{\lambda}}_p^m[k] = \mathbf{0}$ for $k = 1, ..., N-1$, we place this cut into the index set $\{p_0\}$ and denote $\widetilde{\boldsymbol{\nu}}_{p_0} \triangleq \widetilde{\boldsymbol{\nu}}_p^m$, $\widetilde{\boldsymbol{\lambda}}_{p_0} \triangleq \widetilde{\boldsymbol{\lambda}}_p^m$. Similarly, we define index sets $\{p_1\}, ..., \{p_{N-1}\}$ such that for $\{p_i\}$, $\widetilde{\boldsymbol{\nu}}_p[i+1] \neq \mathbf{0}$ or $\widetilde{\boldsymbol{\lambda}}_p[i] \neq \mathbf{0}$, but $\widetilde{\boldsymbol{\nu}}_p[k] = \mathbf{0}$ for $k = i+2, ..., N$, $\widetilde{\boldsymbol{\lambda}}_p[k] = \mathbf{0}$ for $k = i+1, ..., N-1$

Define $\widetilde{\boldsymbol{\Lambda}}_{p_i}$ and $\widetilde{\boldsymbol{\mathcal{V}}}_{p_i}$ according to (24) and (26). Note that $\widetilde{\boldsymbol{\mathcal{V}}}_{p_i}[k] = \mathbf{0}$ for $k = i+1, ..., N-1$, $\widetilde{\boldsymbol{\Lambda}}_{p_i}[k] = \mathbf{0}$ for $k = i+2, ..., N-1$. Define the constant part:

$$S_{p_i} = \sum_{k=0}^{i+1} \widetilde{\boldsymbol{\Lambda}}_{p_i}[k]^T \boldsymbol{\Theta}[k] \tag{45}$$

Therefore, the feasibility cuts can be parsed as:

$$\begin{aligned}
&\widetilde{\boldsymbol{\mathcal{V}}}_{p_0}[0]^T \boldsymbol{\delta}[0] \geq -S_{p_0} && p_0 \in \{p_0\} \\
&\widetilde{\boldsymbol{\mathcal{V}}}_{p_1}[0]^T \boldsymbol{\delta}[0] + \widetilde{\boldsymbol{\mathcal{V}}}_{p_1}[1]^T \boldsymbol{\delta}[1] \geq -S_{p_1} && p_1 \in \{p_1\} \\
&\vdots \\
&\widetilde{\boldsymbol{\mathcal{V}}}_{p_{N-1}}[0]^T \boldsymbol{\delta}[0] + \widetilde{\boldsymbol{\mathcal{V}}}_{p_{N-1}}[1]^T \boldsymbol{\delta}[1] + ... \\
&+ \widetilde{\boldsymbol{\mathcal{V}}}_{p_{N-1}}[N-1]^T \boldsymbol{\delta}[N-1] \geq -S_{p_{N-1}} && p_{N-1} \in \{p_{N-1}\}
\end{aligned} \tag{46}$$

On the other hand, the optimality cuts can be written as:

$$z_0 \geq S_q - \sum_{k=0}^{N-1} \boldsymbol{\mathcal{V}}_q^*[k]^T \boldsymbol{\delta}[k] \quad q \in \{q\} \tag{47}$$

where:

$$S_q \triangleq C_q - \boldsymbol{\Lambda}_q^{*T} \boldsymbol{\Theta} \tag{48}$$

Based on the structure of (46) and (47), we propose an algorithm to solve $\boldsymbol{\delta}[k]$ step by step into the future, using a greedy approach. We first solve $\boldsymbol{\delta}[0]$ by solving the problem at step $k = 0$ denoted by P_0:

$$\begin{aligned}
&\underset{\boldsymbol{\delta}}{\text{minimize}} \quad z_0 \\
\text{s.t.} \quad &\boldsymbol{\delta}[0] \in \{0,1\}^{n_\delta} \\
&\widetilde{\boldsymbol{\mathcal{V}}}_{p_0}[0]^T \boldsymbol{\delta}[0] \geq -S_{p_0} \quad p_0 \in \{p_0\} \\
&z_0 \geq S_q - \boldsymbol{\mathcal{V}}_q^*[0]^T \boldsymbol{\delta}[0] \quad q \in \{q\}
\end{aligned} \tag{49}$$

This one-step problem can be solved using appropriate algorithms, such as Branch and Bound. In many practical cases, the modes within one time-step can be easily enumerated (e.g. quadruped robots have 2^4 contact modes). Solving P_0 is in the worst case checking each mode, and the solving time scales proportional to the number of modes at each time-step. Note if the original master problem is feasible, the first-step problem should be feasible, as the variables and constraints are a subset of the original master problem. Denote the solution by $\boldsymbol{\delta}^*[0]$, which is then substituted into the optimality cuts (47) and the rest of feasibility cuts (46), such that the constant part $S_{p_1}, ..., S_{p_{N-1}}$ and S_q are updated. In the next step, we solve problem P_1, having identical structure as P_0 except that $\widetilde{\boldsymbol{\mathcal{V}}}_{p_0}[0]$, $\boldsymbol{\mathcal{V}}_q^*[0]$ are replaced by $\widetilde{\boldsymbol{\mathcal{V}}}_{p_1}[1]$, $\boldsymbol{\mathcal{V}}_q^*[1]$, respectively, and S_{p_1}, S_q are updated. This procedure is continued to solve $\boldsymbol{\delta}^*[1], ..., \boldsymbol{\delta}^*[N-1]$. Due to the greedy approach, $\boldsymbol{\delta}^*[0]$ does not guarantee the feasibility of P_1. When infeasibility happens, we backtrack the solution from the last step, and pick another less optimal solution. We can also incorporate heuristics of the future constraints at time step k, if bad $\boldsymbol{\delta}[k]$ causes difficulty to solve $\boldsymbol{\delta}[k+1]$. For example, one can include the feasibility cuts at the next iteration by adding constraints:

$$\widetilde{\boldsymbol{\mathcal{V}}}_{p_k}[k]^T \boldsymbol{\delta}[k] + \max_{\boldsymbol{\delta}[k+1]} \{\widetilde{\boldsymbol{\mathcal{V}}}_{p_{k+1}}[k+1]^T \boldsymbol{\delta}[k+1]\} \geq -S_{p_{k+1}} \quad p_{k+1} \in \{p_{k+1}\} \tag{50}$$

Constraint (50) gives the "least amount requirement" for *one* constraint in $\{p_{k+1}\}$ to the previous time step, such that feasibility is guaranteed for *that constraint*. Heuristics may be used to replace the expensive max search. The complete algorithm is provided in Algorithm 4.

Obviously, this algorithm eventually finds a feasible solution if the original master problem is feasible. If backtrack does not happen, the number of solved subproblems grows linearly with respect to the time horizon N. In the worst case, the solving time can still be exponential. We also admit that this greedy algorithm does not guarantee a global optimal solution, as early decisions are made disregarding the optimality down the time horizon. Roughly speaking, early decisions are more essential for control problems, justified by the general decreasing trend on magnitude of Lagrange multipliers. Hence, a greedy approach oftentimes finds high quality solutions in practice.

Despite that Algorithm 4 is simple, we find that it provides high solving speeds for $N \leq 20$ in our experiments. As $N > 20$, the algorithm constantly encounters infeasibility and needs to backtrack. It also finds suboptimal solutions on problems that require early decisions to consider future decisions. In those scenarios, a more complicated mechanism is necessary, perhaps identifying the critical binaries to be solved first. This algorithm can be parallelized by searching multiple sub-optimal solutions at line 5, or warm-started using solutions from previous iterations assuming constraints do not change drastically.

VII. Experiment

We test our Benders MPC algorithm on two different problems: controlling a free-flying robot to move through obstacles, and a cart-pole system to balance with moving soft contact walls. Those problems are also presented as a verification problem in many previous works such as [9], [11], [13], [65], except that the soft contact walls have randomized motion for our tests.

We implement Algorithm 3 to solve this problem. We use $G_a = 0.1$ among the proposed and benchmark methods for all problems. Other important parameters such as I_{max}, K_{feas}, K_{opt}, ϵ, and α are chosen properly and reported for each experiment. For fair comparison with Gurobi's MIQP solver, we use Gurobi's QP solver to solve the Benders

Algorithm 4: Benders Master Problem Solver

Input: $\mathcal{T}_f$, $\mathcal{T}_o$

Initialization iteration $k := 0$
Parse $\mathcal{T}_f$ into (46), and $\mathcal{T}_o$ into (47)
while $k \leq N-1$ **do**
  Solve problem P_k
  if *Feasible* **then**
    Record the optimal $\boldsymbol{\delta}^*[k]$ and cost $z_0[k]$
    $S_q := S_q - \boldsymbol{\mathcal{V}}_q^*[k]^T \boldsymbol{\delta}^*[k], \ \forall q \in \{q\}$
    for $s = k+1, ..., N-1$:
    $S_{p_s} := S_{p_s} + \widetilde{\boldsymbol{\mathcal{V}}}_{p_s}[k]^T \boldsymbol{\delta}^*[k], \ \forall p_s \in \{p_s\}$
    $k := k+1$
  else Infeasible
    repeat
      $k := k-1$
      $S_q := S_q + \boldsymbol{\mathcal{V}}_q^*[k]^T \boldsymbol{\delta}^*[k], \ \forall q \in \{q\}$
      for $s = k+1, ..., N-1$:
      $S_{p_s} := S_{p_s} - \widetilde{\boldsymbol{\mathcal{V}}}_{p_s}[k]^T \boldsymbol{\delta}^*[k], \ \forall p_s \in \{p_s\}$
      if *Other solutions for P_k exist* **then**
        Get a different solution from P_k
      else if *k=0* **then**
        return *Problem infeasible*
    until *Another solution for P_k is found*;
return $\boldsymbol{\delta}^*[0]$, ..., $\boldsymbol{\delta}^*[N-1]$, $m^* = z_0[N-1]$

subproblems. Note that other faster QP solvers listed by [66] can be implemented to further increase the speed. The algorithm is coded in Python, and tested inside a pybullet environment [67] on a 12th Gen Intel Core i7-12800H × 20 laptop with 16GB memory.

For each of the experiment, we report the following:

(i) A representative trajectory with the objective function values, solving speed, number of Benders iterations to find the control, and the number of stored cuts, for each problem along the trajectory.
(ii) A Monte Carlo study showing results collected from 20 randomly generated problems.

The following methods are used for benchmark:

(i) Warm-started Branch and Bound as described by [11], implemented in Python.
(ii) Off-the-shelf solver Gurobi. The problem is set up only once and solved iteratively such that warm-starts are automatically used to minimize the solving time. The default setting is used to optimize the performance.
(iii) GBD without warm-start. We implemented Algorithm 1 such that previous cuts are not used to warm-start the next problem.

The solving time is calculated based on the time when control $(\boldsymbol{\delta}^*, \boldsymbol{u}^*)$ is produced the first time. The extra iterations spent and cuts generated to prove its optimality is not necessary for either applying the control or reproduce the same control in future problems.

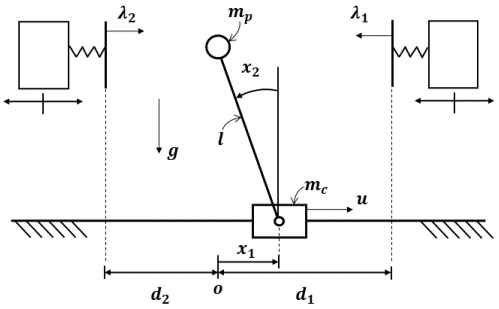

Fig. 1: Cart-pole system with moving soft contact walls.

A. Cart-pole with moving soft contact walls

We studied the problem of controlling a cart-pole system to balance between two moving soft contact walls. The setup is shown in Fig. 1. The state variable $\boldsymbol{x}[k] \in \mathbb{R}^4$ where x_1 is the position of the cart, x_2 is the angle of the pole, and x_3, x_4 are their derivatives. Define $\lambda_1 \geq 0$, $\lambda_2 \geq 0$ as contact forces from the right and the left walls, and f the horizontal actuation force to push the cart. The control input $\boldsymbol{u}[k] = \begin{bmatrix} f & \lambda_1 & \lambda_2 \end{bmatrix}^T \in \mathbb{R}^3$. We linearize the pendulum model around $x_2 = 0$ and discretize with a step size $dt = 0.02s$. Readers are referred to [11] for the complete dynamics of this system.

Two binary variables $\boldsymbol{\delta}[k] \in \mathbb{R}^2$ are defined to describe three contact scenarios: left, right, and no contact. The moving elastic pads are located to the right of the origin at a distance of d_1, and to the left at d_2. Let l be the length of the pole. When the pole penetrates a wall ($x_1 - lcos(x_2) \geq d_1$ or $x_1 - lcos(x_2) \leq -d_2$), additional contact force is generated at the tip of the pole. Otherwise, there is no contact force. This can be modeled as mixed-integer linear constraints:

$$\begin{aligned} \delta_i = 0 \Rightarrow \lambda_i = 0, \ a_i(lx_2 - x_1) + \frac{\lambda_i}{k_i} + d_i \geq 0 \\ \delta_i = 1 \Rightarrow \lambda_i \geq 0, \ a_i(lx_2 - x_1) + \frac{\lambda_i}{k_i} + d_i = 0 \end{aligned} \tag{51}$$

where $i = 1, 2$. $a_1 = 1$ and $a_2 = -1$. k_1 and k_2 are elastic coefficients to model the right and left wall contacts. These logic laws are enforced using the standard big-M approach, where the maximal distance from pole to wall, and maximal contact force are used as big-M constants. Constraints also include the cart position and velocity limits, and pole angle and angular velocity limits. This problem has $n_x = 4$, $n_u = 3$, $n_z = 2$, $n_c = 20$. The objective function penalizes the control efforts, the velocities, and tries to regulate the pole to the zero position.

At the beginning of each test episode, the pendulum begins from a perturbed angle of $x_2 = 10°$ such that it will bump into the wall to regain balance. For the rest of each episode, the persistent random disturbance torque on the pole is generated from a Gaussian distribution $\mathcal{N}(0, 8)$ Nm. The system is constantly disturbed and has to frequently touch the wall for re-balance. The wall motion is generated by a random walk on top of a base sinusoidal motion $\Delta d = 0.03sin(2\pi t) + m$ in which m is from a Brownian motion.

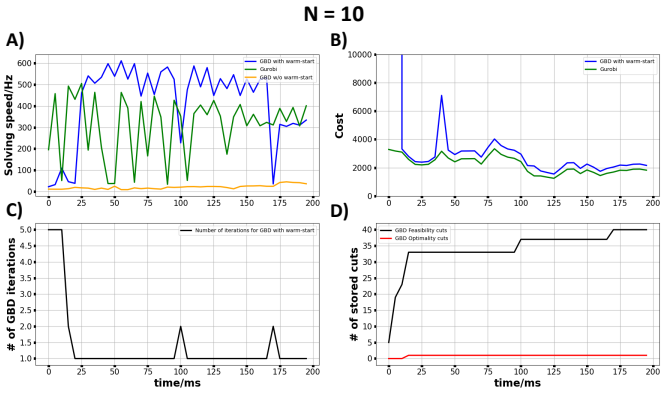

Fig. 2: A case of solving procedure from cold-start when the pole bumps into the moving elastic wall. x-axis is time in ms. A) solving speed comparison among proposed GBD, GBD without warm-start, and Gurobi, y-axis is in Hz. B) Cost of proposed GBD and Gurobi. C) The number of GBD iterations to find control. D) The number of cuts stored during the solving procedure. Blue curves represent proposed GBD algorithm. Green curves represent Gurobi. Orange curve represent GBD without warm-start. For cutting planes, black curve shows the feasibility cuts, red curve shows optimality cuts.

The wall motions are provided to the controller only at runtime through parameter $\boldsymbol{\theta} = \begin{bmatrix} d_1 & d_2 \end{bmatrix}$. For our experiments, we choose mass of cart $1.0kg$, mass of pole $0.4kg$, $l = 0.6m$, $k_1 = k_2 = 50N/m$, control limit $f_{max} = 20N$, and angle limits $\pm\pi/2$. The weights are $\boldsymbol{Q}_k = \text{diag}(1, 50, 1, 50)$, $\boldsymbol{R}_k = 0.1\boldsymbol{I}_3$. The terminal cost $\boldsymbol{Q}_N$ is obtained by solving a discrete algebraic Ricatti equation.

Algorithm 4 is used to solve the master problem. To solve P_k at each time step, we directly evaluate the feasibility and costs for the three contact modes.

Results We experimented with two different planning horizons: 10 and 15. The data is collected from solved problems where at least one contact is planned, removing the cases when contact is not involved. The parameters are $I_{max} = 5$, $K_{feas} = 45$ for $N = 10$, and $I_{max} = 10$, $K_{feas} = 150$ for $N = 15$. K_{opt} is not limited. In addition, $\epsilon = 5000$, and $\alpha = 15°$.

Fig. 2 shows the solving speed in Hz during the first contact in the beginning $200ms$ of an episode. The solver begins from cold-start but has to plan contact ever since $t = 0$. In the first few iterations of cold-start, Algorithm 3 cannot find any feasible solution and output zero control. After the cold-start phase, the algorithm starts to output control, and the solving speed increases over Gurobi. Note that the solving speed remains on average $10Hz$ without warm-start shown by the orange curve in subfigure A in Fig. 2. The cost of Algorithm 3 is only slightly worse to Gurobi due to no control in the first few iterations. If I_{max} is not limited, it gets identical solutions to Gurobi. We highlight the data efficiency of Algorithm 3 from the subfigures C, D showing less than 50 cuts can already provide good warm-starts for the initial conditions encountered along the trajectory. After the cold-start phase, GBD only picks up new cuts once a while, as shown by the number of GBD iterations (subfigure C). On the other hand, the neural-network classifier proposed by [13] consumes over 90000 solved problems offline trying to parametrically resolve the same problem.

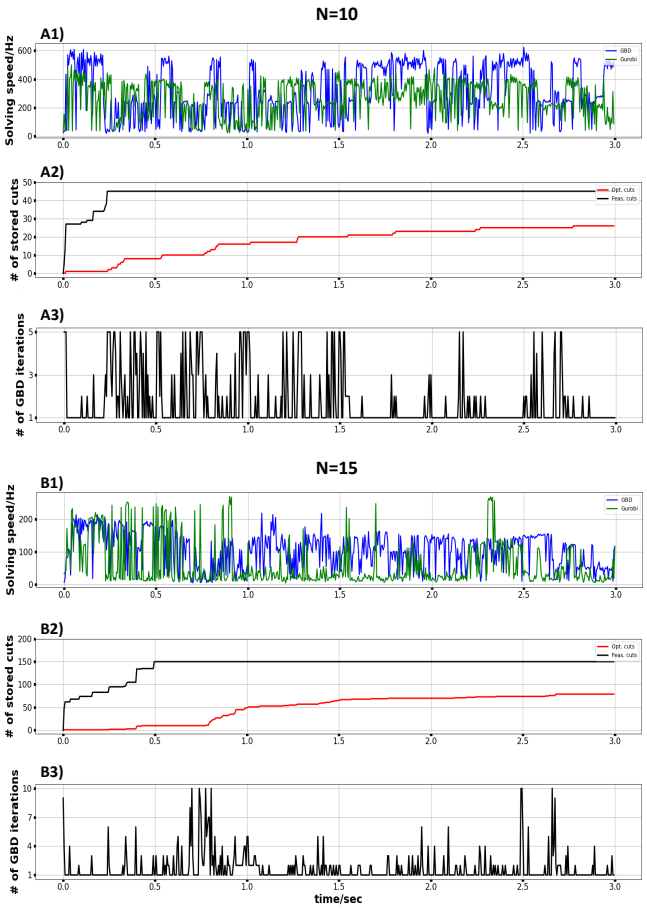

Fig. 3: Solving speed, number of stored cuts, and number of GBD iterations for $N = 10$ and $N = 15$ on cart-pole with contact experiment. Figures A1, A2, A3 show N=10. Figure A1 shows the solving speed of GBD (blue curve) compared against Gurobi (green curve) in Hz. A2 shows the number of stored feasibility cuts (black curve) and optimality cuts (red curve). A3 shows the number of GBD iterations. Figures B1, B2, B3 show the same results for N=15.

We run the Monte-Carlo experiment for the scenario described above and collect 20 trajectories under random wall motions and disturbance torques, benchmark against the warm-started B&B algorithm. Fig. 4 gives the histogram result showing the number of GBD iterations and their frequencies. Thanks to the warm-start, 99.2% of problem instances are solved within 5 iterations, except for a few problems during the cold-start phase. On the other hand, the Branch and Bound algorithm relies on subproblems. The warm-start scheme reduces the number of solved subproblems over 50%. However, the BB solver still goes through more than $10\times$ subproblems to converge compared to the GBD solver, from our averaged data.

Aside from the experiment for $200ms$, we also run the algorithm for longer than 1 minute until the number of cuts converge. Fig. 3 plots the solving speed and number of cuts for 3 seconds, when at least one contact is planned. Using a finite buffer avoids storing too many cuts and maintains the solving speed while still preventing cold-starts from frequently happening. This is justified by 77% of the cases and 74% cases resolved within one GBD iteration for $N = 10$ and $N = 15$. The solving speed of GBD is also

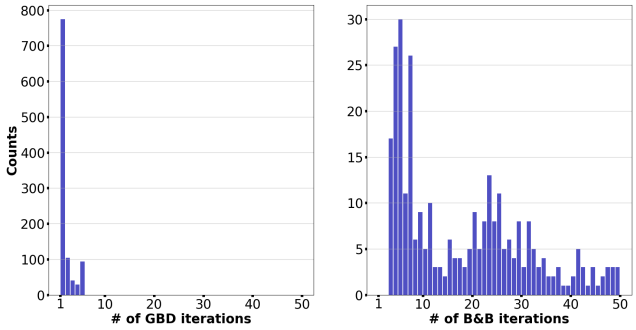

Fig. 4: Comparison of number of solver iterations for different problems of $(\boldsymbol{x}_{ini}, \boldsymbol{\theta})$. x-axis is the range of solver iterations. y axis is the count of problem instances from the collected trajectories. Left: The proposed GBD with continual learning. Right: Branch and Bound with warm-start [11].

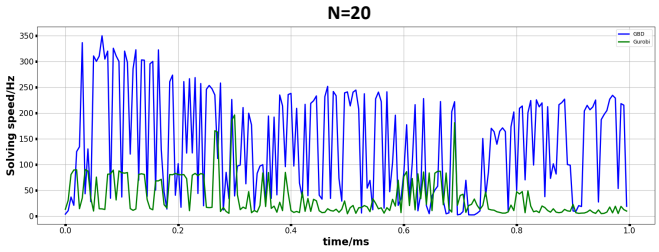

Fig. 5: solving speed for cart-pole during contact at N=20. The blue curve shows Algorithm 3 but solves master problem with Gurobi. The green curve shows directly solving MIQP with Gurobi.

competent with Gurobi, and exceeds Gurobi if one iteration resolves the problem. For $N = 10$, 40% of the complete solving time is used on sub-QPs, and 14% is used on master problems (Algorithm 4), while 48% on sub-QPs, and 17% on master problems for $N = 15$.

However, Algorithm 4 becomes less effective at $N = 20$, constantly backtracking to find different solutions. This causes more than 60% of the solving time spent on the master problem. Better master problem solver is required to scale to longer time horizons. We can instead use Gurobi to solve the master problem which still often exceeds the speed of directly using Gurobi to solve MIQP (Fig. 5), showing the effectiveness of Algorithm 3. For this problem, over 50% cases are resolved within the presolve stage.

B. Free-flying robot obstacle avoidance

We studied the problem of a point mass robot flying through 2-D obstacles to reach the goal following linear dynamics. Three examples are shown by subfigures A1, B1, C1 in Fig. 6. The state variables $\boldsymbol{x}[k] \in \mathbb{R}^4$ include the 2-D positions x, y and velocities $\dot{x}$, $\dot{y}$. The controls $\boldsymbol{u}[k] \in \mathbb{R}^2$ are x and y direction pushing forces. We define two binary variables $\boldsymbol{\delta}[t] \in \mathbb{R}^2$ to enforce obstacle avoidance. Each obstacle is modeled as a square with its exterior regions divided into four linearly bounded regions $\mathcal{R}_{e,1}, \mathcal{R}_{e,2}, \mathcal{R}_{e,3}, \mathcal{R}_{e,4}$ available for the robot to traverse. The obstacle avoidance constraints enforce that $(x, y) \in \mathcal{R}_{e,1}$, $\mathcal{R}_{e,2}$, $\mathcal{R}_{e,3}$, $\mathcal{R}_{e,4}$ under $\boldsymbol{\delta}_i[t] = 00,\ 01,\ 10,\ 11$, respectively. These are enforced by mixed-binary linear constraints through the standard big-M approach. The constraints include obstacle avoidance, state and control limits. Let M_o be the number of obstacles, and this problem has $n_x = 4$, $n_u = 2$, $n_\delta = 2M_o$, $n_c = 4M_o + 8$. The objective function penalizes the Euclidean distance to the goal and the amount of control.

The task of our hybrid MPC is to generate controls for the robot to reach a target among obstacles under disturbance forces. For our experiment, we select robot mass 1kg, control limit 30N in both x and y directions. The discretization step size $dt = 0.02s$. The obstacles are first generated at uniform grid points then altered randomly, to avoid crowding within a small region. The width of obstacles d_o follows Gaussian distribution $d_o \sim \mathcal{N}(0.7, 0.05)$ meters. The target position has uniformly generated x position and the y position is set beyond all the obstacles. The amount of noise μ follows $\mu \sim \mathcal{N}(0, 10)$ Newtons in both x and y directions. For the objective function, we choose $\boldsymbol{Q}_k = \text{diag}(100, 100, 1, 1)$, $\boldsymbol{R}_k = \boldsymbol{I}_2$. The terminal cost $\boldsymbol{Q}_N$ is obtained by solving a discrete algebraic Ricatti equation.

We again used Algorithm 4 to solve the master problem. To solve P_k at each time step, we populate a list of all possible binary solutions for one time step offline. This is done by first gridding the space, then going over each grid point and identifying the collision free region $\mathcal{R}_{e,i}$ for each obstacle. P_k is solved by directly evaluating the feasibility and costs for modes in the list. To reduce the number of backtracks, we use (50) to incorporate feasibility cuts one step ahead.

Results We experimented on the number of obstacles 3, 6, 9, with planned steps 9, 12, 15, representing an increasing scale of the problem. The parameters are $I_{max} = 15$, $K_{feas} = 50$ for $N = 9$, $I_{max} = 80$, $K_{feas} = 150$ for $N = 12$, and $I_{max} = 200$, $K_{feas} = 700$ for $N = 15$. K_{opt} is not limited. In addition, $\epsilon = 5000$, and $\alpha = 15°$. All results are compiled in Fig. 6.

The sub-figures A3, B3, and C3 in Fig. 6 show the solving speed, optimal cost, number of GBD iterations and number of stored cuts for the trajectory around 3, 6, and 9 obstacles. We also conducted a Monte Carlo study for this problem and collected 20 trajectories under random obstacle positions, target positions and disturbances. The results are shown by sub-figure A2, B2, and C2 in Fig. 6. The solving speed is slower compared to Gurobi, yet remains competitive. A nontrivial portion of time is consumed by processing the cuts. According to the Monte Carlo experiment, sub-QPs and master problems take only 15% and 17% of the total solving time for N=9, 18% and 29% for N=12, and 12% and 37% for N=15. A C++ implementation is expected to significantly increase the solving speeds. We once again highlight the data efficiency of our algorithm. The sub-figures A5, B5, and C5 of Fig. 6 show less than 300 stored cuts can already provide good warm-starts for the specific initial condition. GBD only picks up new cuts once a while after the cold-start phase as demonstrated by the curves of GBD iterations and the histograms. This is in contrast with over 90000 offline solved problems in [13], trying to parametrically resolve the problem.

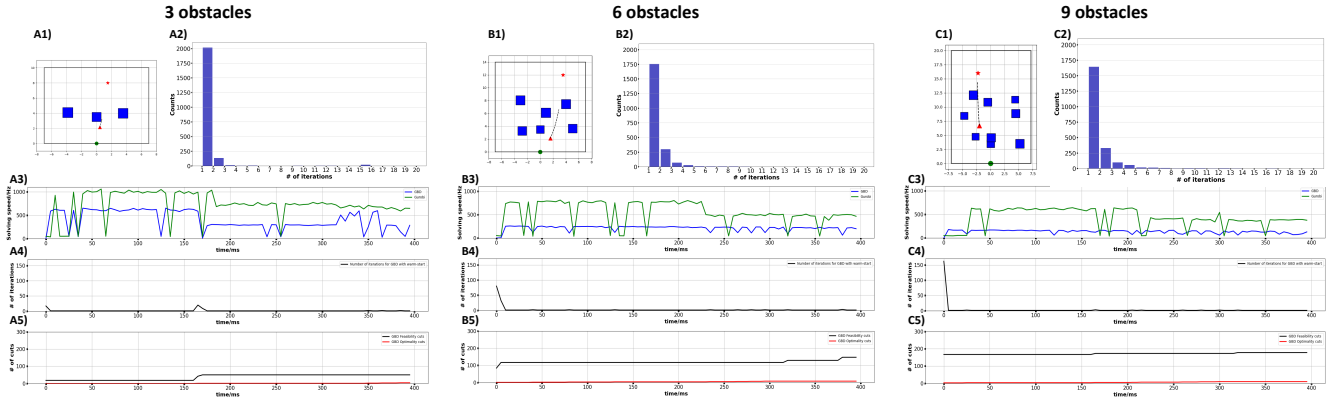

Fig. 6: Results for free-flying robots navigating around 3, 6, and 9 obstacles. Sub-figure A1, B1, C1 show examples of planned trajectories. The initial position is shown by green dot, target position by red star, current position by red triangle, planned trajectory in a black dashed line, and obstacles by blue squares. Sub-figure A3-A5, B3-B5, C3-C5 show solving speed, number of GBD iterations, and number of stored cuts, corresponding to A1, B1, C1. Sub-figure A2, B2, C2 show histograms for the number of GBD iterations generated by Monte Carlo experiments.

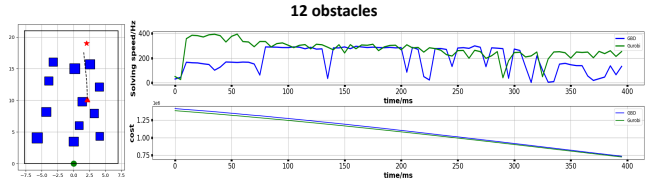

Fig. 7: Left: Free-flying robot problem under $M_o = 12$, $N = 20$. Right up: solving speeds. Right down: optimal costs.

Similar to the cart-pole experiment, Algorithm 4 becomes less effective when $N \geq 20$. We use Gurobi to solve the master problem for $M_o = 12$, $N = 20$. The solving speeds and costs shown on the right of Fig. 7. Over 30% cases are resolved within the presolve stage. The solving speed largely matches Gurobi, despite more than 50% solving time spent on processing the cuts.

VIII. Conclusion, Discussion and Future Work

In this paper, we proposed a hybrid MPC algorithm based on Generalized Benders decomposition with continual learning. The algorithm stores cutting planes from the invariant dual space of the subproblems inside a finite buffer. After a short cold-start phase, the stored cuts provide warm-starts for the new problem instances to increase the solving speed. We also proposed a simple yet effective algorithm leveraging sparse feasibility cuts to solve the master problem. We show competitive solving speeds with commercialized solver Gurobi in controlling the cart-pole system with randomly moving soft walls, and free-flying robots navigating through obstacles.

A. Comparison with other approaches

1) Comparison with Branch and Bound: The Branch and Bound approach construct a large number of subproblems. By querying those subproblems, the algorithm uses heuristics to decide which binary branches have potentially smaller costs. GBD avoids using subproblems. It instead enumerates a large number of cuts, and superimpose them to build the cost map. While those cuts can still be computationally expensive, our proposed algorithm leverages on the sparsity of feasibility cuts to alleviate this burden. When subproblems are expensive to solve, GBD may give faster solving speed. On the other hand, Branch and Bound benefits from rich heuristics based on the subproblems.

2) Comparison with ADMM: Both ADMM and GBD belong to the class of dual decomposition methods. ADMM uses a primal-dual update procedure, which is simple but widely applicable to QPs, MIPs, or even MINLPs. On the other hand, GBD requires discovering the problem structure and identifying complicating variables. The subproblems are ideally convex and satisfy strong duality so the bounds are tighter. Despite its simplicity, ADMM does not build a representation of the invariant dual. As a result, it is difficult to learn from a large number of previously solved problems to build warm-starts. As [9] shows, the non-warm-started ADMM can take multiple iterations to converge. Shifting the contact sequence in time can generate warm-starts, but may break down under disturbances or randomly changing environments. In addition, ADMM generally lacks convergence guarantees for MIP problems as GBD does. Its convergence on MIP or hybrid nonlinear problems depends on the weights hence very problem-specific.

3) Comparison with other data-driven approach: Several previous works such as [25], [27], [58] proposed storing data online and using the K-nearest neighbor approach to retrieve data for warm-starts. The warm-starts for mode sequence $\boldsymbol{\delta}_i$ are retrieved based on an increasing order of distance measure $d(\boldsymbol{\Theta}, \boldsymbol{\Theta}_i)$ of current parameter $\boldsymbol{\Theta}$ and stored parameters $\{\boldsymbol{\Theta}_i\}$. Since this approach does not store any internal structure of the problem, especially the infeasible trials, it is limited to retrieving warm-starts one-by-one. As a result, it only works well when there is plenty of data (see the theoretical analysis of [58]). On the other hand, our algorithm takes cuts from both feasible and infeasible trials and superimposes them, hence more data efficient.

Due to the fast cold-start, even if the system dynamics are only known at run-time or completely change, the time cost to learn new dynamics for our problem is at the scale of hundreds of milliseconds. This is much faster than training

neural-network-based policies [3], [13]. This learning procedure can potentially be carried out online such that the robot quickly learns during the trying process to deal with untrained scenarios before it goes unstable.

B. Combining online learning with prior knowledge

Despite that our algorithm works for relatively smaller scale problems, it is not expected to scale to very large problems as the number of necessary cuts increases fast. It makes sense to combine this approach with prior knowledge obtained offline, such as heuristics based branching strategies, or trained neural-network. They can maintain the speed when GBD goes through cold-starts. On the other hand, the branching heuristics obtained offline may not work well in problems outside their validation set, where GBD can improve their performance. GBD can also be used to automatically tighten the relaxations, compatible with many relaxation based methods such as Graph of convex set [68].

C. Stability analysis

The general idea to prove stability for MPCs is to use the objective function as the Lyapunov function. If we can find a control that is "good enough", we can guarantee stability by the decrease of cost. For our GBD algorithm, since the master problem uses a relaxed version of the cost map, the real subQP cost may not be as good as the master problem expects. However, we can still prove stability if the gap is small enough. This general idea has been proposed in previous works under the subject named sub-optimal model predictive control [20], [69]–[72].

Therefore, one does not have to wait until finishing collecting data to implement the control. As the algorithm proceeds, the applied control keeps on improving. The algorithm hopefully finds a stabilizing control before the system drops into a region where no such control exists. Verifying this kind of stability for the continually learned controllers is a future work.

D. Other future works

An obvious future work is to test our algorithm on nonlinear programs or hybrid nonlinear programs. In fact, the complicating variable $\boldsymbol{\delta}$ does not necessarily need to be discrete, but can be continuous and involved in nonlinear constraints. Additionally, GBD can also be combined with Branch and Bound, resulting in Branch and Benders cut, which combines the power of Benders cuts and subproblems. Finally, we would like to evaluate our continual learning scheme on real hardware.

Appendix I
Partial change of system dynamics

Assume the dynamics constraint can be written as:

$$\begin{bmatrix}\boldsymbol{A}_1 & \boldsymbol{A}_2(\boldsymbol{\phi})\end{bmatrix}\begin{bmatrix}\boldsymbol{x}_1\\ \boldsymbol{x}_2\end{bmatrix} = \boldsymbol{b}(\boldsymbol{x}_{in}, \boldsymbol{\delta}) \tag{52}$$

where $\boldsymbol{\phi}$ represent the part of system dynamics that changes randomly due to environment or disturbance force. The inequality constraints should also be separated similarly:

$$\begin{bmatrix}\boldsymbol{C}_1 & \boldsymbol{C}_2\end{bmatrix}\begin{bmatrix}\boldsymbol{x}_1\\ \boldsymbol{x}_2\end{bmatrix} = \boldsymbol{d}(\boldsymbol{\theta}, \boldsymbol{\delta}) \tag{53}$$

The subproblem becomes:

$$\begin{aligned} v(\boldsymbol{\Theta}, \boldsymbol{\delta}, \boldsymbol{x}_2) = \underset{\boldsymbol{x}_1}{\text{minimize}} \quad & ||\boldsymbol{x} - \boldsymbol{x}_g||_{\boldsymbol{Q}}^2 \\ \text{s.t.} \quad & \boldsymbol{A}_1\boldsymbol{x}_1 = \boldsymbol{b}(\boldsymbol{x}_{in}, \boldsymbol{\delta}) - \boldsymbol{A}_2(\boldsymbol{\phi})\boldsymbol{x}_2 \\ & \boldsymbol{C}_1\boldsymbol{x}_1 \leq \boldsymbol{d}(\boldsymbol{\theta}, \boldsymbol{\delta}) - \boldsymbol{C}_2\boldsymbol{x}_2 \end{aligned} \tag{54}$$

The master problem becomes:

$$\begin{aligned} \underset{\boldsymbol{\delta},\ \boldsymbol{x}_2}{\text{minimize}} \quad & v(\boldsymbol{\Theta}, \boldsymbol{\delta}, \boldsymbol{x}_2) \\ \text{s.t.} \quad & \boldsymbol{\delta}_k \in \{0, 1\} \\ & \boldsymbol{\delta},\ \boldsymbol{x}_2 \in V(\boldsymbol{\Theta}) \end{aligned} \tag{55}$$

The parameter $\boldsymbol{\Theta}$ includes $\boldsymbol{x}_{in}$, $\boldsymbol{\theta}$, $\boldsymbol{\phi}$. This would rely on the dynamics constraints being separable into the form of (52), which may require proper coordinate transformations.

While the subQP remains mostly unchanged, the master problem now includes continuous variables $\boldsymbol{x}_2$. The proposed algorithm is still applicable in this case. The feasibility cuts and optimality cuts are updated with additional $\boldsymbol{A}_2(\boldsymbol{\phi})\boldsymbol{x}_2$ and $\boldsymbol{C}_2\boldsymbol{x}_2$ terms.

Appendix II
Treating rank deficient objective function

If $\boldsymbol{Q}_k$ are not positive definite but semi-definite, the inverse of $\boldsymbol{Q}$ does not exist. The dual (17) needs to be reformulated. Some extra implicit constraints on $(\boldsymbol{\nu}^*, \boldsymbol{\lambda}^*)$ need to be imposed. Define orthogonal transformation matrix $\boldsymbol{T}$ that diagonalizes $\boldsymbol{Q}$, such that $\boldsymbol{T}^{-1}\boldsymbol{Q}\boldsymbol{T} = \widehat{\boldsymbol{Q}}$. Also let $\widehat{\boldsymbol{x}} = \boldsymbol{T}^{-1}\boldsymbol{x}$, $\widehat{\boldsymbol{x}}_g = \boldsymbol{T}^{-1}\boldsymbol{x}_g$, $\widehat{\boldsymbol{A}} = \boldsymbol{A}\boldsymbol{T}$, $\widehat{\boldsymbol{C}} = \boldsymbol{C}\boldsymbol{T}$. The Lagrangian of the subproblem (14) needs to be bounded below for the dual to be well-defined. Let $\{j\}$ be the set of zero rows in $\widehat{\boldsymbol{Q}}$. For any $j \in \{j\}$, row j of $\widehat{\boldsymbol{A}}^T\boldsymbol{\nu}^* + \widehat{\boldsymbol{C}}^T\boldsymbol{\lambda}^* + \widehat{\boldsymbol{Q}}\widehat{\boldsymbol{x}}_g$ should also be zero, or:

$$(\boldsymbol{A}^T\boldsymbol{\nu}^*)_j + (\boldsymbol{C}^T\boldsymbol{\lambda}^*)_j = 0 \quad \forall j \in \{j\} \tag{56}$$

If this is indeed the case, (17) is re-written such that row j's in $\boldsymbol{Q}$, $\boldsymbol{\lambda}$, $\boldsymbol{\nu}$ are removed from the objective, and the additional constraint (56) is added to its feasible set. When subQPs are solved, the returned dual variables should satisfy this constraint. Since this constraint is invariant under $\boldsymbol{\Theta}$, the same lower bound arguments can apply.

Appendix III
Proof of lemma 1

We present a proof of Lemma 1. Recall the Farkas' lemma (Theorem 4.6 in [54]):

Theorem 5. *Let $\tilde{\boldsymbol{A}} \in \mathbb{R}^{m\times n}$ and $\tilde{\boldsymbol{b}} \in \mathbb{R}^m$. Then, exactly one of the two following alternatives holds:*

1) *There exists some $\tilde{\boldsymbol{x}} \geq \boldsymbol{0}$ such that $\tilde{\boldsymbol{A}}\tilde{\boldsymbol{x}} = \tilde{\boldsymbol{b}}$.*
2) *There exists some vector $\tilde{\boldsymbol{p}}$ such that $\tilde{\boldsymbol{p}}^T\tilde{\boldsymbol{A}} \geq \boldsymbol{0}^T$ and $\tilde{\boldsymbol{p}}^T\tilde{\boldsymbol{b}} < 0$.*

For any vector $\boldsymbol{x}$, there exists $\boldsymbol{y} \geq \boldsymbol{0}$, $\boldsymbol{z} \geq \boldsymbol{0}$ such that $\boldsymbol{x} = \boldsymbol{y} - \boldsymbol{z}$. The inequality constraint $\boldsymbol{C}\boldsymbol{x} \leq \boldsymbol{d}$ is equivalent to $\boldsymbol{C}\boldsymbol{x} + \boldsymbol{\delta} = \boldsymbol{d}, \exists \boldsymbol{\delta} \geq \boldsymbol{0}$. Hence the first condition of Lemma 1 is equivalent to the existence of $\tilde{\boldsymbol{x}} = \begin{bmatrix} \boldsymbol{y}^T & \boldsymbol{z}^T & \boldsymbol{\delta}^T \end{bmatrix}^T \geq 0$ such that:

$$\underbrace{\begin{bmatrix} \boldsymbol{A} & -\boldsymbol{A} & \boldsymbol{0} \\ \boldsymbol{C} & -\boldsymbol{C} & \boldsymbol{I} \end{bmatrix}}_{\tilde{\boldsymbol{A}}} \underbrace{\begin{bmatrix} \boldsymbol{y} \\ \boldsymbol{z} \\ \boldsymbol{\delta} \end{bmatrix}}_{\tilde{\boldsymbol{x}}} = \underbrace{\begin{bmatrix} \boldsymbol{b} \\ \boldsymbol{d} \end{bmatrix}}_{\tilde{\boldsymbol{b}}} \tag{57}$$

By Theorem 5, this condition is alternative to the existence of $\tilde{\boldsymbol{p}} = \begin{bmatrix} \boldsymbol{y}^T & \boldsymbol{z}^T \end{bmatrix}^T$ such that $\tilde{\boldsymbol{p}}^T \tilde{\boldsymbol{A}} \geq \boldsymbol{0}^T$ and $\tilde{\boldsymbol{p}}^T \tilde{\boldsymbol{b}} < 0$, which gives the second condition of Lemma 1.

Appendix IV
Proof of Lemma 4

We prove lemma 4 leveraging on the results of [24] to compute the Lipschitz constant. First, we write down the state variables as functions of control inputs:

$$\boldsymbol{x}[k] = \boldsymbol{E}^k \boldsymbol{x}_{in} + \sum_{j=0}^{k-1} \boldsymbol{E}^j (\boldsymbol{F}\boldsymbol{u}[k-1-j] + \boldsymbol{G}\boldsymbol{\delta}[k-1-j]) \tag{58}$$

Plug (58) into the objective function and inequality constraints in the subQP (14), we reformulate the problem as:

$$\begin{aligned} v(\boldsymbol{\Theta}, \boldsymbol{\delta}) &= \boldsymbol{x}_{in}^T \boldsymbol{M}_x \boldsymbol{x}_{in} + \boldsymbol{x}_{in}^T \boldsymbol{M}_{x\delta} \boldsymbol{\delta} + \boldsymbol{\delta}^T \boldsymbol{M}_\delta \boldsymbol{\delta} \\ &+ \min_{\boldsymbol{U}} \ \boldsymbol{U}^T \boldsymbol{M}_u \boldsymbol{U} + (\boldsymbol{x}_{in}^T \boldsymbol{M}_{xu} + \boldsymbol{\delta}^T \boldsymbol{M}_{\delta u}) \boldsymbol{U} \\ &\text{s.t.} \ \ \boldsymbol{N}_u \boldsymbol{U} \leq \boldsymbol{N}_\theta \boldsymbol{\Theta} + \boldsymbol{N}_\delta \boldsymbol{\delta} \end{aligned} \tag{59}$$

where $\boldsymbol{U} \triangleq \begin{bmatrix} \boldsymbol{u}[0]^T & \boldsymbol{u}[1]^T & \cdots & \boldsymbol{u}[N-1]^T \end{bmatrix}^T \in \mathbb{R}^{N n_u}$. The matrices $\boldsymbol{M}_x$, $\boldsymbol{M}_u$, $\boldsymbol{M}_\delta$, $\boldsymbol{M}_{xu}$, $\boldsymbol{M}_{\delta u}$, $\boldsymbol{M}_{x\delta}$, $\boldsymbol{N}_\theta$, $\boldsymbol{N}_u$, $\boldsymbol{N}_\delta$ are easily obtained from $\boldsymbol{E}$, $\boldsymbol{F}$, $\boldsymbol{G}$, $\boldsymbol{H}_1$, $\boldsymbol{H}_2$, $\boldsymbol{H}_3$. For simplicity, we set $\boldsymbol{x}_g[k] = \boldsymbol{0}$. Define variable transformation $\boldsymbol{z} = \boldsymbol{U} + \frac{1}{2}\boldsymbol{M}_u^{-1}\boldsymbol{M}_{xu}^T \boldsymbol{x}_{in} + \frac{1}{2}\boldsymbol{M}_u^{-1}\boldsymbol{M}_{\delta u}^T \boldsymbol{\delta}$, and objective function:

$$\begin{aligned} v_z(\boldsymbol{x}_{in}, \boldsymbol{\theta}, \boldsymbol{\delta}) &= v(\boldsymbol{\Theta}, \boldsymbol{\delta}) \\ &- \boldsymbol{x}_{in}^T \boldsymbol{M}_x \boldsymbol{x}_{in} - \boldsymbol{x}_{in}^T \boldsymbol{M}_{x\delta} \boldsymbol{\delta} - \boldsymbol{\delta}^T \boldsymbol{M}_\delta \boldsymbol{\delta} \\ &+ \frac{1}{4} (\boldsymbol{x}_{in}^T \boldsymbol{M}_{xu} + \boldsymbol{\delta}^T \boldsymbol{M}_{\delta u}) \boldsymbol{M}_u^{-1} (\boldsymbol{M}_{xu}^T \boldsymbol{x}_{in} + \boldsymbol{M}_{\delta u}^T \boldsymbol{\delta}) \end{aligned} \tag{60}$$

The QP part of (59) can be written as:

$$\begin{aligned} v_z(\boldsymbol{x}_{in}, \boldsymbol{\theta}, \boldsymbol{\delta}) = \min_{\boldsymbol{z}} \ & \boldsymbol{z}^T \boldsymbol{M}_u \boldsymbol{z} \\ \text{s.t.} \ & \boldsymbol{N}_u \boldsymbol{z} \leq \boldsymbol{W}_\theta \boldsymbol{\Theta} + \boldsymbol{W}_\delta \boldsymbol{\delta} \end{aligned} \tag{61}$$

where $\boldsymbol{W}_\theta$, $\boldsymbol{W}_\delta$ can be obtained from $\boldsymbol{M}_{xu}$, $\boldsymbol{M}_u$, $\boldsymbol{N}_x$, $\boldsymbol{N}_u$, $\boldsymbol{N}_\delta$. For the inequality constraints in (61), let the active constraints be $\widetilde{\boldsymbol{N}}_u \boldsymbol{z} = \widetilde{\boldsymbol{W}}_\theta \boldsymbol{\Theta} + \widetilde{\boldsymbol{W}}_\delta \boldsymbol{\delta}$, such that inequality constraints are removed. Assume $\widetilde{\boldsymbol{N}}_u$ has linearly independent rows. Utilizing the first order Karush-Kuhn-Tucker (KKT) optimality conditions, we can solve:

$$\boldsymbol{z} = \boldsymbol{M}_u^{-1} \widetilde{\boldsymbol{N}}_u^T (\widetilde{\boldsymbol{N}}_u \boldsymbol{M}_u^{-1} \widetilde{\boldsymbol{N}}_u^T)^{-1} (\widetilde{\boldsymbol{W}}_\theta \boldsymbol{\Theta} + \widetilde{\boldsymbol{W}}_\delta \boldsymbol{\delta}) \tag{62}$$

which is a piecewise affine with respect to $\boldsymbol{x}_{in}, \boldsymbol{\theta}, \boldsymbol{\delta}$, and the objective function is a piecewise quadratic function. The matrices $\widetilde{\boldsymbol{N}}_u$, $\widetilde{\boldsymbol{W}}_x$, $\widetilde{\boldsymbol{W}}_\theta$, $\widetilde{\boldsymbol{W}}_\delta$ depend on the active set. If the active set does not change, we can write the Lipschitz constant in closed-form. By mean-value theorem, there exist a point $\begin{bmatrix} \boldsymbol{\Theta}_0^T & \boldsymbol{\delta}_0^T \end{bmatrix}$ on the line segment between $\begin{bmatrix} \boldsymbol{\Theta}_1^T & \boldsymbol{\delta}_1^{*T} \end{bmatrix}$ and $\begin{bmatrix} \boldsymbol{\Theta}_2^T & \boldsymbol{\delta}_2^{*T} \end{bmatrix}$, such that:

$$\begin{aligned} &|v(\boldsymbol{\Theta}_2, \boldsymbol{\delta}_2^*) - v(\boldsymbol{\Theta}_1, \boldsymbol{\delta}_1^*)| \leq \\ &\quad 2 || \begin{bmatrix} \boldsymbol{\Theta}_0^T & \boldsymbol{\delta}_0^T \end{bmatrix} \boldsymbol{\mathcal{H}} ||_2 || \begin{bmatrix} \Delta\boldsymbol{\Theta}^T & \Delta\boldsymbol{\delta}^{*T} \end{bmatrix} ||_2 \end{aligned} \tag{63}$$

The definition of $\boldsymbol{\mathcal{H}}$ can be obtained through plugging (62) into (60), and write $v(\boldsymbol{\Theta}, \boldsymbol{\delta}^*)$ into the second order form:

$$v(\boldsymbol{\Theta}, \boldsymbol{\delta}^*) = \begin{bmatrix} \boldsymbol{\Theta}^T & \boldsymbol{\delta}^{*T} \end{bmatrix} \boldsymbol{\mathcal{H}} \begin{bmatrix} \boldsymbol{\Theta}^T & \boldsymbol{\delta}^{*T} \end{bmatrix}^T \tag{64}$$

References

[1] S. Kuindersma, R. Deits, M. Fallon, A. Valenzuela, H. Dai, F. Permenter, T. Koolen, P. Marion, and R. Tedrake, "Optimization-based locomotion planning, estimation, and control design for the atlas humanoid robot," *Autonomous robots*, vol. 40, pp. 429–455, 2016.

[2] X. Lin, J. Zhang, J. Shen, G. Fernandez, and D. W. Hong, "Optimization based motion planning for multi-limbed vertical climbing robots," in *2019 IEEE/RSJ International Conference on Intelligent Robots and Systems (IROS)*. IEEE, 2019, pp. 1918–1925.

[3] F. R. Hogan and A. Rodriguez, "Reactive planar non-prehensile manipulation with hybrid model predictive control," *The International Journal of Robotics Research*, vol. 39, no. 7, pp. 755–773, 2020.

[4] J. Zhang, X. Lin, and D. W. Hong, "Transition motion planning for multi-limbed vertical climbing robots using complementarity constraints," in *2021 IEEE International Conference on Robotics and Automation (ICRA)*. IEEE, 2021, pp. 2033–2039.

[5] A. Bemporad and M. Morari, "Control of systems integrating logic, dynamics, and constraints," *Automatica*, vol. 35, no. 3, pp. 407–427, 1999.

[6] W. Heemels, J. M. Schumacher, and S. Weiland, "Linear complementarity systems," *SIAM journal on applied mathematics*, vol. 60, no. 4, pp. 1234–1269, 2000.

[7] E. Sontag, "Nonlinear regulation: The piecewise linear approach," *IEEE Transactions on automatic control*, vol. 26, no. 2, pp. 346–358, 1981.

[8] W. P. Heemels, B. De Schutter, and A. Bemporad, "Equivalence of hybrid dynamical models," *Automatica*, vol. 37, no. 7, pp. 1085–1091, 2001.

[9] A. Aydinoglu, A. Wei, and M. Posa, "Consensus complementarity control for multi-contact mpc," *arXiv preprint arXiv:2304.11259*, 2023.

[10] S. L. Cleac'h, T. Howell, M. Schwager, and Z. Manchester, "Fast contact-implicit model-predictive control," *arXiv preprint arXiv:2107.05616*, 2021.

[11] T. Marcucci and R. Tedrake, "Warm start of mixed-integer programs for model predictive control of hybrid systems," *IEEE Transactions on Automatic Control*, vol. 66, no. 6, pp. 2433–2448, 2020.

[12] A. M. Geoffrion, "Generalized benders decomposition," *Journal of optimization theory and applications*, vol. 10, pp. 237–260, 1972.

[13] A. Cauligi, P. Culbertson, E. Schmerling, M. Schwager, B. Stellato, and M. Pavone, "Coco: Online mixed-integer control via supervised learning," *IEEE Robotics and Automation Letters*, vol. 7, no. 2, pp. 1447–1454, 2021.

[14] R. Deits, T. Koolen, and R. Tedrake, "Lvis: Learning from value function intervals for contact-aware robot controllers," in *2019 International Conference on Robotics and Automation (ICRA)*. IEEE, 2019, pp. 7762–7768.

[15] A. Cauligi, P. Culbertson, B. Stellato, D. Bertsimas, M. Schwager, and M. Pavone, "Learning mixed-integer convex optimization strategies for robot planning and control," in *2020 59th IEEE Conference on Decision and Control (CDC)*. IEEE, 2020, pp. 1698–1705.

[16] L. Xuan, "Generalized benders decomposition with continual learning for hybrid model predictive control in dynamic environment," *arXiv preprint arXiv:2310.03344*, 2023.

[17] J. Tobajas, F. Garcia-Torres, P. Roncero-Sánchez, J. Vázquez, L. Bellatreche, and E. Nieto, "Resilience-oriented schedule of microgrids with hybrid energy storage system using model predictive control," *Applied Energy*, vol. 306, p. 118092, 2022.

[18] Y. Cao, Z. Zhang, F. Cheng, and S. Su, "Trajectory optimization for high-speed trains via a mixed integer linear programming approach," *IEEE Transactions on Intelligent Transportation Systems*, vol. 23, no. 10, pp. 17 666–17 676, 2022.

[19] M. Klaučo, J. Drgoňa, M. Kvasnica, and S. Di Cairano, "Building temperature control by simple mpc-like feedback laws learned from closed-loop data," *IFAC Proceedings Volumes*, vol. 47, no. 3, pp. 581–586, 2014.

[20] T. Marcucci, R. Deits, M. Gabiccini, A. Bicchi, and R. Tedrake, "Approximate hybrid model predictive control for multi-contact push recovery in complex environments," in *2017 IEEE-RAS 17th International Conference on Humanoid Robotics (Humanoids)*. IEEE, 2017, pp. 31–38.

[21] A. M. Geoffrion, "Lagrangian relaxation for integer programming," *50 Years of Integer Programming 1958-2008: From the Early Years to the State-of-the-Art*, pp. 243–281, 2010.

[22] M. Anitescu, "On using the elastic mode in nonlinear programming approaches to mathematical programs with complementarity constraints," *SIAM Journal on Optimization*, vol. 15, no. 4, pp. 1203–1236, 2005.

[23] R. Lazimy, "Mixed-integer quadratic programming," *Mathematical Programming*, vol. 22, pp. 332–349, 1982.

[24] A. Bemporad, M. Morari, V. Dua, and E. N. Pistikopoulos, "The explicit linear quadratic regulator for constrained systems," *Automatica*, vol. 38, no. 1, pp. 3–20, 2002.

[25] J.-J. Zhu and G. Martius, "Fast non-parametric learning to accelerate mixed-integer programming for hybrid model predictive control," *IFAC-PapersOnLine*, vol. 53, no. 2, pp. 5239–5245, 2020.

[26] X. Lin, G. I. Fernandez, and D. W. Hong, "Reduce: Reformulation of mixed integer programs using data from unsupervised clusters for learning efficient strategies," in *2022 International Conference on Robotics and Automation (ICRA)*. IEEE, 2022, pp. 4459–4465.

[27] X. Lin, F. Xu, A. Schperberg, and D. Hong, "Learning near-global-optimal strategies for hybrid non-convex model predictive control of single rigid body locomotion," *arXiv preprint arXiv:2207.07846*, 2022.

[28] P. Hespanhol, R. Quirynen, and S. Di Cairano, "A structure exploiting branch-and-bound algorithm for mixed-integer model predictive control," in *2019 18th European Control Conference (ECC)*. IEEE, 2019, pp. 2763–2768.

[29] B. Stellato, G. Banjac, P. Goulart, A. Bemporad, and S. Boyd, "Osqp: An operator splitting solver for quadratic programs," *Mathematical Programming Computation*, vol. 12, no. 4, pp. 637–672, 2020.

[30] Y. Shirai, X. Lin, A. Schperberg, Y. Tanaka, H. Kato, V. Vichathorn, and D. Hong, "Simultaneous contact-rich grasping and locomotion via distributed optimization enabling free-climbing for multi-limbed robots," in *2022 IEEE/RSJ International Conference on Intelligent Robots and Systems (IROS)*. IEEE, 2022, pp. 13 563–13 570.

[31] X. Lin, G. I. Fernandez, Y. Liu, T. Zhu, Y. Shirai, and D. Hong, "Multi-modal multi-agent optimization for limms, a modular robotics approach to delivery automation," in *2022 IEEE/RSJ International Conference on Intelligent Robots and Systems (IROS)*. IEEE, 2022, pp. 12 674–12 681.

[32] B. Wu and B. Ghanem, "ℓ_p-box admm: A versatile framework for integer programming," *IEEE transactions on pattern analysis and machine intelligence*, vol. 41, no. 7, pp. 1695–1708, 2018.

[33] J. Benders, "Partitioning procedures for solving mixed-variables programming problems ‘," *Numerische mathematik*, vol. 4, no. 1, pp. 238–252, 1962.

[34] G. B. Dantzig and P. Wolfe, "Decomposition principle for linear programs," *Operations research*, vol. 8, no. 1, pp. 101–111, 1960.

[35] L. J. Watters, "Reduction of integer polynomial programming problems to zero-one linear programming problems," *Operations Research*, vol. 15, no. 6, pp. 1171–1174, 1967.

[36] F. Glover, "Improved linear integer programming formulations of nonlinear integer problems," *Management science*, vol. 22, no. 4, pp. 455–460, 1975.

[37] R. McBride and J. Yormark, "An implicit enumeration algorithm for quadratic integer programming," *Management Science*, vol. 26, no. 3, pp. 282–296, 1980.

[38] J. N. Hooker and H. Yan, "Logic circuit verification by benders decomposition," *Principles and practice of constraint programming: the newport papers*, pp. 267–288, 1995.

[39] J. N. Hooker and G. Ottosson, "Logic-based benders decomposition," *Mathematical Programming*, vol. 96, no. 1, pp. 33–60, 2003.

[40] G. Codato and M. Fischetti, "Combinatorial benders' cuts for mixed-integer linear programming," *Operations Research*, vol. 54, no. 4, pp. 756–766, 2006.

[41] J. R. Birge and F. Louveaux, *Introduction to stochastic programming*. Springer Science & Business Media, 2011.

[42] P.-D. Moroşan, R. Bourdais, D. Dumur, and J. Buisson, "A distributed mpc strategy based on benders' decomposition applied to multi-source multi-zone temperature regulation," *Journal of Process Control*, vol. 21, no. 5, pp. 729–737, 2011.

[43] R. Rahmaniani, T. G. Crainic, M. Gendreau, and W. Rei, "The benders decomposition algorithm: A literature review," *European Journal of Operational Research*, vol. 259, no. 3, pp. 801–817, 2017.

[44] W. Rei, J.-F. Cordeau, M. Gendreau, and P. Soriano, "Accelerating benders decomposition by local branching," *INFORMS Journal on Computing*, vol. 21, no. 2, pp. 333–345, 2009.

[45] A. M. Costa, J.-F. Cordeau, B. Gendron, and G. Laporte, "Accelerating benders decomposition with heuristicmaster problem solutions," *Pesquisa Operacional*, vol. 32, pp. 03–20, 2012.

[46] T. L. Magnanti and R. T. Wong, "Accelerating benders decomposition: Algorithmic enhancement and model selection criteria," *Operations research*, vol. 29, no. 3, pp. 464–484, 1981.

[47] J.-F. Cordeau, G. Stojković, F. Soumis, and J. Desrosiers, "Benders decomposition for simultaneous aircraft routing and crew scheduling," *Transportation science*, vol. 35, no. 4, pp. 375–388, 2001.

[48] J. A. Rodríguez, M. F. Anjos, P. Côté, and G. Desaulniers, "Accelerating benders decomposition for short-term hydropower maintenance scheduling," *European Journal of Operational Research*, vol. 289, no. 1, pp. 240–253, 2021.

[49] A. Grothey, S. Leyffer, and K. McKinnon, "A note on feasibility in benders decomposition," *Numerical Analysis Report NA/188, Dundee University*, 1999.

[50] M. V. Pereira and L. M. Pinto, "Stochastic optimization of a multireservoir hydroelectric system: A decomposition approach," *Water resources research*, vol. 21, no. 6, pp. 779–792, 1985.

[51] ——, "Multi-stage stochastic optimization applied to energy planning," *Mathematical programming*, vol. 52, pp. 359–375, 1991.

[52] J. Warrington, P. N. Beuchat, and J. Lygeros, "Generalized dual dynamic programming for infinite horizon problems in continuous state and action spaces," *IEEE Transactions on Automatic Control*, vol. 64, no. 12, pp. 5012–5023, 2019.

[53] S. Menta, J. Warrington, J. Lygeros, and M. Morari, "Learning q-function approximations for hybrid control problems," *IEEE Control Systems Letters*, vol. 6, pp. 1364–1369, 2021.

[54] D. Bertsimas and J. N. Tsitsiklis, *Introduction to linear optimization*. Athena scientific Belmont, MA, 1997, vol. 6.

[55] L. Wu and M. Shahidehpour, "Accelerating the benders decomposition for network-constrained unit commitment problems," *Energy Systems*, vol. 1, no. 3, pp. 339–376, 2010.

[56] N. Beheshti Asl and S. MirHassani, "Accelerating benders decomposition: multiple cuts via multiple solutions," *Journal of Combinatorial Optimization*, vol. 37, pp. 806–826, 2019.

[57] G. Optimization. (2023) Mipgap. [Online]. Available: https://www.gurobi.com/documentation/9.5/refman/mipgap2.html

[58] K. Hauser, "Learning the problem-optimum map: Analysis and application to global optimization in robotics," *IEEE Transactions on Robotics*, vol. 33, no. 1, pp. 141–152, 2016.

[59] V. Dua and E. N. Pistikopoulos, "An algorithm for the solution of multiparametric mixed integer linear programming problems," *Annals of operations research*, vol. 99, pp. 123–139, 2000.

[60] H. J. Ferreau, H. G. Bock, and M. Diehl, "An online active set strategy to overcome the limitations of explicit mpc," *International Journal of Robust and Nonlinear Control: IFAC-Affiliated Journal*, vol. 18, no. 8, pp. 816–830, 2008.

[61] M. Walter, "Sparsity of lift-and-project cutting planes," in *Operations Research Proceedings 2012: Selected Papers of the International An-*

nual Conference of the German Operations Research Society (GOR), Leibniz University of Hannover, Germany, September 5-7, 2012. Springer, 2013, pp. 9–14.

[62] L. Alfandari, I. Ljubić, and M. D. M. da Silva, "A tailored benders decomposition approach for last-mile delivery with autonomous robots," *European Journal of Operational Research*, vol. 299, no. 2, pp. 510–525, 2022.

[63] S. S. Dey, M. Molinaro, and Q. Wang, "Analysis of sparse cutting planes for sparse milps with applications to stochastic milps," *Mathematics of Operations Research*, vol. 43, no. 1, pp. 304–332, 2018.

[64] T. Marcucci, M. Petersen, D. von Wrangel, and R. Tedrake, "Motion planning around obstacles with convex optimization," *arXiv preprint arXiv:2205.04422*, 2022.

[65] R. Quirynen and S. Di Cairano, "Tailored presolve techniques in branch-and-bound method for fast mixed-integer optimal control applications," *Optimal Control Applications and Methods*, vol. 44, no. 6, pp. 3139–3167, 2023.

[66] S. Caron, D. Arnström, S. Bonagiri, A. Dechaume, N. Flowers, A. Heins, T. Ishikawa, D. Kenefake, G. Mazzamuto, D. Meoli, B. O'Donoghue, A. A. Oppenheimer, A. Pandala, J. J. Quiroz Omaña, N. Rontsis, P. Shah, S. St-Jean, N. Vitucci, S. Wolfers, @bdelhaisse, @MeindertHH, @rimaddo, @urob, and @shaoanlu, "qpsolvers: Quadratic Programming Solvers in Python," Dec. 2023. [Online]. Available: https://github.com/qpsolvers/qpsolvers

[67] E. Coumans and Y. Bai, "Pybullet, a python module for physics simulation for games, robotics and machine learning," 2016.

[68] T. Marcucci, J. Umenberger, P. A. Parrilo, and R. Tedrake, "Shortest paths in graphs of convex sets," *arXiv preprint arXiv:2101.11565*, 2021.

[69] D. Q. Mayne, J. B. Rawlings, C. V. Rao, and P. O. Scokaert, "Constrained model predictive control: Stability and optimality," *Automatica*, vol. 36, no. 6, pp. 789–814, 2000.

[70] P. O. Scokaert, D. Q. Mayne, and J. B. Rawlings, "Suboptimal model predictive control (feasibility implies stability)," *IEEE Transactions on Automatic Control*, vol. 44, no. 3, pp. 648–654, 1999.

[71] C. N. Jones and M. Morari, "Approximate explicit mpc using bilevel optimization," in *2009 European control conference (ECC)*. IEEE, 2009, pp. 2396–2401.

[72] M. N. Zeilinger, C. N. Jones, and M. Morari, "Real-time suboptimal model predictive control using a combination of explicit mpc and online optimization," *IEEE Transactions on Automatic Control*, vol. 56, no. 7, pp. 1524–1534, 2011.